

NZ
RAC 2601
(PCD-TR-64-17)

Design Summary Report
HIGH RESPONSE, LOW LEVEL
THRUST MEASUREMENT SYSTEM

Contract NAS 5-9029



FAIRCHILD HILLER
REPUBLIC AVIATION DIVISION
FARMINGDALE, LONG ISLAND, NEW YORK

FACILITY FORM 602

N69-77997

(ACCESSION NUMBER)

7783

(PAGES)

Cr #165944

(NASA CR OR TMX OR AD NUMBER)

(THRU)

Done

(CODE)

(CATEGORY)

RAC 2601
(PCD-TR-64-17)
24 September 1964

Design Summary Report
HIGH RESPONSE, LOW LEVEL
THRUST MEASUREMENT SYSTEM

Contract NAS 5-9029

RAC 2601

Prepared for
National Aeronautics and Space Administration
Goddard Space Flight Center
Greenbelt, Maryland

REPUBLIC AVIATION DIVISION
FAIRCHILD HILLER CORPORATION
Farmingdale, L. I., New York

PROPRIETARY INFORMATION

Reproduction, dissemination or use of information contained herein is prohibited without prior written approval of Republic Aviation Corporation. All use by or with approval of the U. S. Government is anticipated.

CONTENTS

<u>SECTION</u>		<u>PAGE</u>
I	INTRODUCTION	1
II	STATEMENT OF THE PROBLEM	5
III	ANALYSIS	8
	A. Systems Considerations	8
	B. Displacement and Force Transducers	14
	C. Vibration Isolation	28
	D. Error Analysis - Thermal Expansion	35
	E. Calibration	39
IV	THRUST STAND CONFIGURATIONS-RECOMMENDATIONS	46
	A. Vibration Analysis	46
	B. Test Package Support	49
	C. Transducer Location and Support	51
	D. Forcer Motor	52
	E. Calibration	56
	F. Supply Line and Feed Through	56
	G. Control Console	57
V	REFERENCES	58

APPENDIX

ILLUSTRATIONS

		<u>PAGE</u>
III-A-1	Block Diagram - Open Loop (1)	9
III-A-2	Block Diagram - Closed Loop (2)	11
III-A-3	Block Diagram - Closed Loop (3)	13
III-B-1	Capacitor Transducer	24
III-B-2	Transducer-Diagram	25
III-B-3	Bridge Circuit - Schematic	26
III-C-1	Vibration Isolation - Schematic	29
III-C-2	Frequency Response Modification	32
III-C-3	Pulse Distortion	32
III-C-4	Compensation Network	34
III-D-1	Thermal Expansion Error Diagram	36
III-E-1	Steady State Calibrator	40
III-E-2	Dynamic Calibrator Subsystem	43
IV-A-1	Thrust Stand Diagram	47
IV-D-1	Forcer Motor	54
PC036D0000	General Arrangement Drawing of Thrust Stand (Enclosure)	
PC031D0000	Perspective Drawing of Thrust Stand (Enclosure)	

SECTION I

INTRODUCTION

This Design Summary Report is presented in satisfaction of Phase I of Contract NAS 5-9029, issued by the Goddard Space Flight Center of the National Aeronautics and Space Administration.

The objective of the contract is primarily to develop a high response thrust stand, capable of assessing the thrust performance of small, attitude control thrusters applied to space vehicles.

A secondary objective is to ensure that the thrust stand system, with thruster system mounted, can be used in conjunction with a computer to simulate a closed loop attitude control system for vehicles undertaking various space missions.

The contract required that the first three-month period be spent in the study of the problems of low-level thrust measurement in the Goddard test facility, the definition of several methods of measuring such thrust and the quantitative assessment of the potentials of these methods to satisfy the requirements.

This Design Report is the result, therefore, of the first three months study period of the contract. The theoretical analysis of problem areas, such as the selection of control loop type, loop analysis, isolation from known background vibration and the influence of a changing temperature environment are presented; certain sensor and loop systems are suggested, quantitative performance assessments of sensors, loops and other stand components are given.

One of the items of major importance in the development of the thrust system is seen to be the motion or force transducer. Because of

the importance of this item, and because of the stringent requirements that the design of the system places upon it, an industry survey was made of low level thrust stands and the transducers suitable for use on such stands.

Basic target parameters for the stand were generated and can be laid down as follows:

- 1) To support a test thruster package of up to 4 pounds.
- 2) The stand natural frequency to be equal to, or better than, 250 cycles per second, while loaded with the 4 pound package.
- 3) To measure, with an overall system accuracy of 5%, thrust in the range of 5 millipounds to 200 millipounds.
- 4) The system to include built-in and remotely operated steady state and dynamic calibrators, referable to an NBS standard.
- 5) Following upon the test package weight, frequency requirement and thrust resolution, the motion transducer to have a threshold figure of 3×10^{-9} inches.
- 6) The stand to contain built-in isolation of background vibration down to 10 cycles per second. This isolation to be primarily in the direction of the thrust axis, but isolation to be provided against cross talk coupling from other axes.

From the analyses and the investigations made it is concluded that the development of such a thrust measuring system is just within the borders of the present state-of-the-art.

The main area in question is undoubtedly the transducer-loop combination, where experience in the sensing, and scaling to meaningful force values, of such small motions as those involved in this application is extremely limited.

However, this is not the only area calling for evaluation; the effects of temperature change, background vibrations, resonant vibrations set up in stand structure, test equipment settling and many other points must be given careful consideration.

Recommendations for the approach to the development of the thrust system

are given in the report and can be generally summarized as follows.

Three types of transducers are known that will sense the motions called for and at the force levels specified. One form of sensor, the piezoelectric, is seen as only being applicable if the thrust is limited to a pulsed form. The two remaining types, differential transformer and capacitor, can be used to measure long-term steady thrusts with high response characteristics. The differential transformer is solely a displacement sensor and for the proposed application would have to be used with a closed loop system. The capacitor transducer, as typified by a unit at present under investigation at Republic Aviation Corporation, can be used in open loop or closed loop systems. Inherent in the capacitor transducer is the ability to combine the force restraint element with the motion sensing element, seen as an absolute essential for the application of an open loop system to the proposed system. It is required, however, that the transducer of an open loop system be linear and virtually free of drift and hysteresis. The capacitor sensor is also applicable to a closed loop system, and in fact in such a system the sensor is relieved of its linearity requirements and less restricted in its drift and hysteresis parameters.

Additionally, it is known from the theoretical studies presented here. that the damping for a suitable open loop system is such as to require some feed-back amplification circuit, if an impractically large unit is to be avoided.

To ensure that the system has the ability to accept an alternative transducer, to provide the flexibility to compensate for insufficient sensor linearity or drift or hysteresis and to provide the damping levels required, it has been recommended that the system be conceived as a closed loop system. The system configuration has been developed on this basis, with the understanding that the proving of the capacitor transducer, in linearity, etc., can simplify the system to an open loop with the damping amplifier network.

Temperature environment is an important consideration in this system, and the affect of it upon the transducer and other stand components has been

studied. The stand configuration recommended is consequently designed to reduce the temperature change effects to a small proportion of the overall accuracy of the system.

At the beginning of this Design Analysis, the test facility at Goddard, into which the proposed stand will be integrated, was studied; together with a vibration survey of the facility. It was concluded during this initial study that, as the background vibrations were emanating from so many pieces of support equipment and the facility was integrated in such a manner, it was impractical to insert any vibration isolation prior to the test chamber. The thrust stand has been designed therefore to incorporate its own vibration isolation, making it a flexible piece of equipment able to operate in facilities other than that for which it was originally intended.

Although the thrust measuring system will be designed with a band width of 250 cps this does not automatically restrict the accuracy of thrust measurement to that frequency range. Since the thrust stand dynamic parameters will be well known and established, it is possible to correct recorded thrust measurements for the high frequency thrust stand errors. Computational methods for accomplishing this are discussed in the Appendix.

SECTION II

STATEMENT OF THE PROBLEM

The most basic requirements of the thrust stand as stated by the Work Statement are the following:

- a) Thrust range - 5 to 200 millipounds force
- b) Accuracy and resolution - better than 5% (of which 2% can be assigned as transducer accuracy). Thus, for the most sensitive range scale it is necessary to resolve a "minimum bit" of 0.10 millipound.
- c) Thrustor weight - 4 pounds (plus 1 pound for mounting platform)
- d) Required frequency response - 250 cycles/second.

These elements of the specification coupled with the knowledge of the temperature, vacuum and vibration environment have important implications which form the basis for the design and evaluation studies. Considered within this report are discussions and recommendations with respect to the type of detector, the damping techniques available, the relationship between the basic spring restraint necessary for 250 cps and the possibilities of additional mechanical resonances, threshold detection, overall accuracy, noise sources, open versus closed loop operation, temperature effects, vibration isolation, calibration techniques, magnetic field effects, and long term drift.

Thrust measurement may be accomplished by many techniques, but regardless of which is selected the basic sensor is one making a displacement measurement. The specification implies the scale of displacements to be considered. Examination of several options shows this.

Calibrated Spring: One can obtain the measure of a force by the deflection of a calibrated spring. In this case the mass associated with the thrustor and its mounting will resonate with the spring. The specified mass, $\frac{5}{32.2}$ slugs, and the frequency (250 cps or higher) define a minimum spring rate $K = (2\pi f)^2 m = 0.383 \times 10^6$ lb/ft. This spring rate and the least significant force "bit" of 0.10×10^{-3} lbs define a minimum displacement which must be sensed; this displacement is

$$\frac{0.10 \times 10^{-3}}{0.383 \times 10^6} = 0.26 \times 10^{-9} \text{ ft or } 3.1 \times 10^{-9} \text{ inches}$$

Thus, displacements smaller than 0.01 microinch must be sensed.

Accelerometer: Conceptually one might consider sensing a force by measuring the acceleration produced. However, when one considers that the acceleration can only be that produced by 0.10 millipound on a 5 pound mass, and that the measurement must be faster than 1 millisecond to obtain a suitable speed of response (250 cps) one finds again that displacements of less than 0.01 microinch must be detected with some accuracy.

It will be found that any other concept, such as the frequency measurement of a vibrating string, or a force balance system where an opposing force is generated to balance the applied force, results in essentially the same requirement; namely a measuring element capable of resolving displacements smaller than 0.01 microinch, with an inherent stiffness such that a resonant frequency higher than 250 cps is obtained.

Therefore, the thrust measurement problem will be solved within the constraints of about 4×10^5 lb/ft stiffness and a displacement sensitivity of about 10^{-8} inch.

The type of sensor is critical and must be selected on the basis of accuracy, threshold, linearity, short term and long term drift, sensitivity, frequency response, sensitivity to environment and whether the system is open-ended or a closed loop. Tests have been made on a capacitive sensor which indicates that the basic resolution can be met. Drift levels must be determined and this is expected to help confirm the present conclusion that closed loop operation is most suited to the needs of the system. Drift and low frequency noise are discriminated against in a closed loop and a separate damper is not required, if an electronic spring is used, as network damping may be employed. Another sensor being tested is a piezoelectric device which does not have the sensitivity in its present form but is expected to permit an open loop operation based on its linearity relatively noise free output and stiffness of over 35×10^6 lb/ft.

The overall accuracy must be considered in the light of expansion effects due to temperature, hysteresis of the spring restraint, long term verses short term sensor drift, calibration technique, effect of the loop and noise sources as they are introduced either mechanically or electrically. All are interconnected and while

many are not critical they must be included in component's specifications. Others, such as the thermal expansion must be handled by a specific design approach which is discussed in the report.

External mechanical vibration as sensed by the displacement sensor must be reduced to a value consistent with the overall accuracy requirements without the reduction of the performance of the measurement system. In addition, as the frequency response is 250 cps, the design must be such as to provide an extremely stiff mount between the sensor and the actual thruster under test so as to avoid any deterioration in frequency response as measured by the thrust stand. Resonant modes in other axes must be avoided as well, as they may cross-couple into the sensor, creating another noise source.

Magnetic and electromagnetic fields will be present and must be reviewed in the light of the sensor sensitivity to these fields, shielding techniques, and displacements of the stand during the operation. It is presently considered that standard design techniques will eliminate this as a source of difficulty.

The basic calibration approach is described and error sources considered. The threshold or resolution is related to the system requirements and the accuracy is referred back to a standard NBS weight. Such problems as weight changes in a vacuum, differential thermal expansion, hysteresis and backlash are all covered. The A.C. calibration is included and is primarily to demonstrate the frequency response over the required frequency range.

The sum total of these considerations coupled with the detailed mechanical and electrical design results in an overall system which will meet the basic requirements.

SECTION III

ANALYSIS

A. SYSTEMS CONSIDERATIONS

There are several possible systems concepts in building a high response, low thrust measurement system. As discussed in Section II any such system ultimately relies on a displacement sensor and some equivalent of a stiff spring. In detail many variations are possible. Three configurations have been specifically analyzed and are:

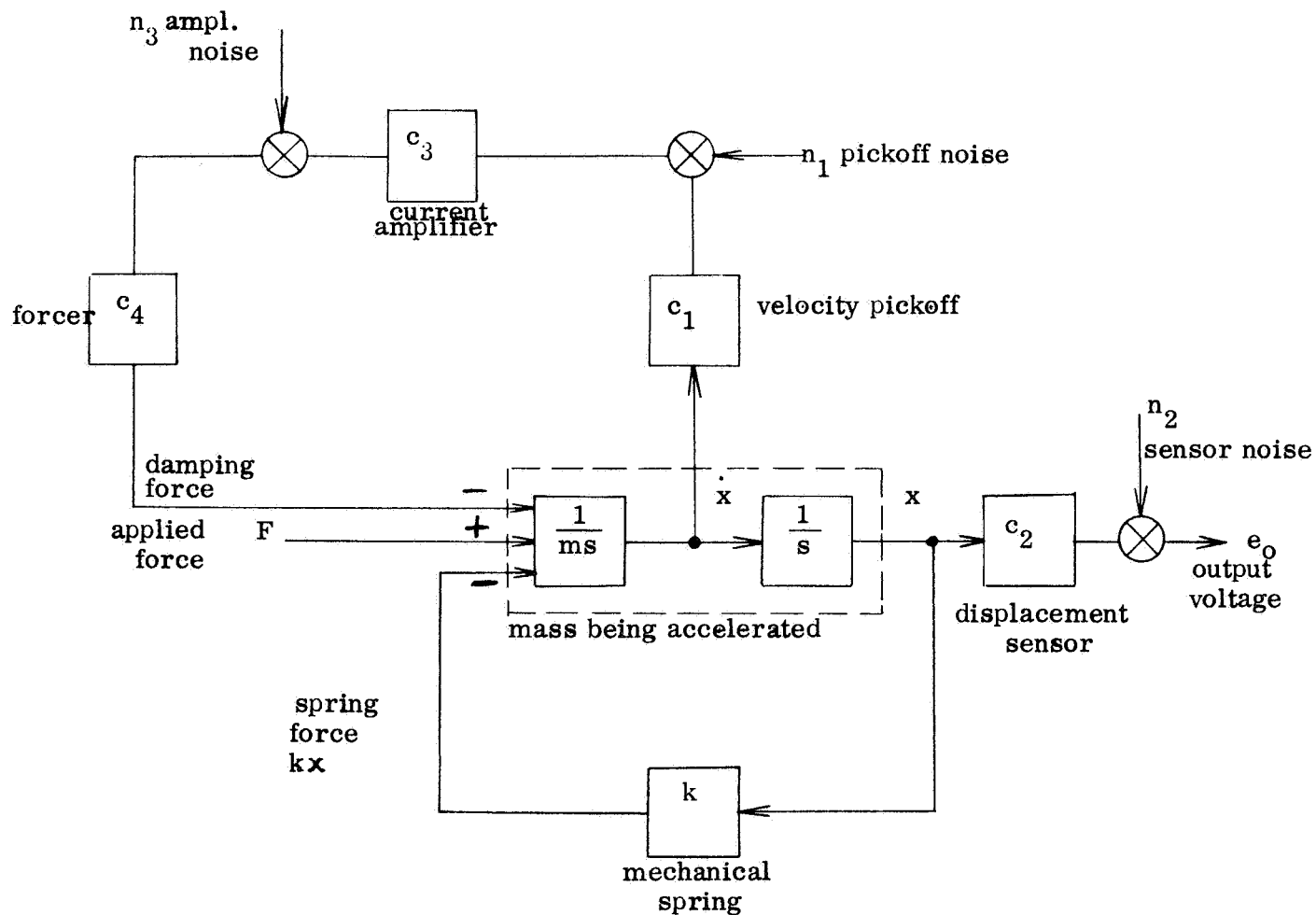
- 1) Mechanical spring restraint, electromagnetic damping
- 2) Electromagnetic spring, closed loop, with network damping
- 3) Electromagnetic spring, closed loop, electromagnetic damping

All three of these imply a sensor capable of accurate resolution of very small displacements. In system (1) the displacement is controlled by a very stiff mechanical spring; in (2) and (3) the electrical signal detected by the sensor is amplified and used to drive a force coil so as to produce at all times a force equal and opposite to the applied thrust. To avoid strong resonances it is necessary to add damping to these devices. Direct viscous damping cannot be produced in adequate amounts at such minute displacements, hence all three schemes use derived electrical damping signals, applied to force coils which produce properly phased damping forces. The specific loop arrangements, as discussed below, differ in manner in which stray signals (noise) are amplified or attenuated as well as being different with regard to the actual equipment required.

1. System 1 - Mechanical Spring Restraint, Electromagnetic Damping

A block diagram of this system is shown on Figure III-A-1, indicating the dynamics of the mass/spring system, as well as the electromagnetic damping loop. From inspection of the loop, it is apparent that the response to input forces and noise voltages is

$$x = \frac{F + C_3 C_4 N_1 + C_4 N_3}{ms^2 + C_1 C_3 C_4 s + K} = \frac{F + C_3 C_4 N_1 + C_4 N_3}{K(1 + 2\sigma \frac{s}{\Omega} + \frac{s^2}{\Omega^2})}$$



- $m = 5/32.2$ slugs
 $k = .383 \cdot 10^6$ lb/ft
 $c_2 =$ output scale factor, volts/ft
 $c_1 =$ velocity pickoff scale factor volts/(ft/sec)
 $c_3 =$ current amplifier transconductance, amperes/volt
 $c_4 =$ forcer scale factor, lbs/amperes

Figure III-A-1: Block Diagram - System (1)
 Mechanical Spring Restraint -
 Electromagnetic Damping

$$e_o = C_2 x + N_2$$

One observes that:

- a) Displacement sensor noise and drift appears directly at the output.
- b) Only noise components of N_1 and N_3 above the system frequency (250 cps) are attenuated. Low frequency noise (below 250 cps) appears as an input force.
- c) For adequate damping ($\sigma \approx 0.6$) one must have $C_1 C_3 C_4 = \frac{2\sigma}{\Omega} K = 293 \text{ lbs (ft/sec)}$.
- d) The current amplifier may be an A.C. amplifier; it is not necessary to provide D.C. damping currents to obtain a stable system. However it is desired to have a bandpass of the amplifier to extend from about 1 or 2 cps to beyond 5000 cps.
- e) The spring rate must be approximately $4 \times 10^5 \text{ lb/ft}$.
- f) The sensitivity of the detector and associated amplifier must be of the order of $4 \times 10^6 \text{ volts/ft}$ to provide adequate signal level for recording purposes.

2. System 2 - Electromagnetic Spring, Closed Loop, with Network Damping

This system is shown in block diagram on Figure III-A-2. The response to the applied force and noise voltages for this system is

$$e_o = \frac{F \frac{C_2}{m} (s + \beta) + N_2 s^2 (s + \beta) - N_3 \frac{C_2 C_4}{m} (s + \beta) - N_4 \frac{n}{C_5} (s + \alpha)}{s^3 + \beta s^2 + ns + n\alpha}$$

where the lead network corner frequencies are selected as

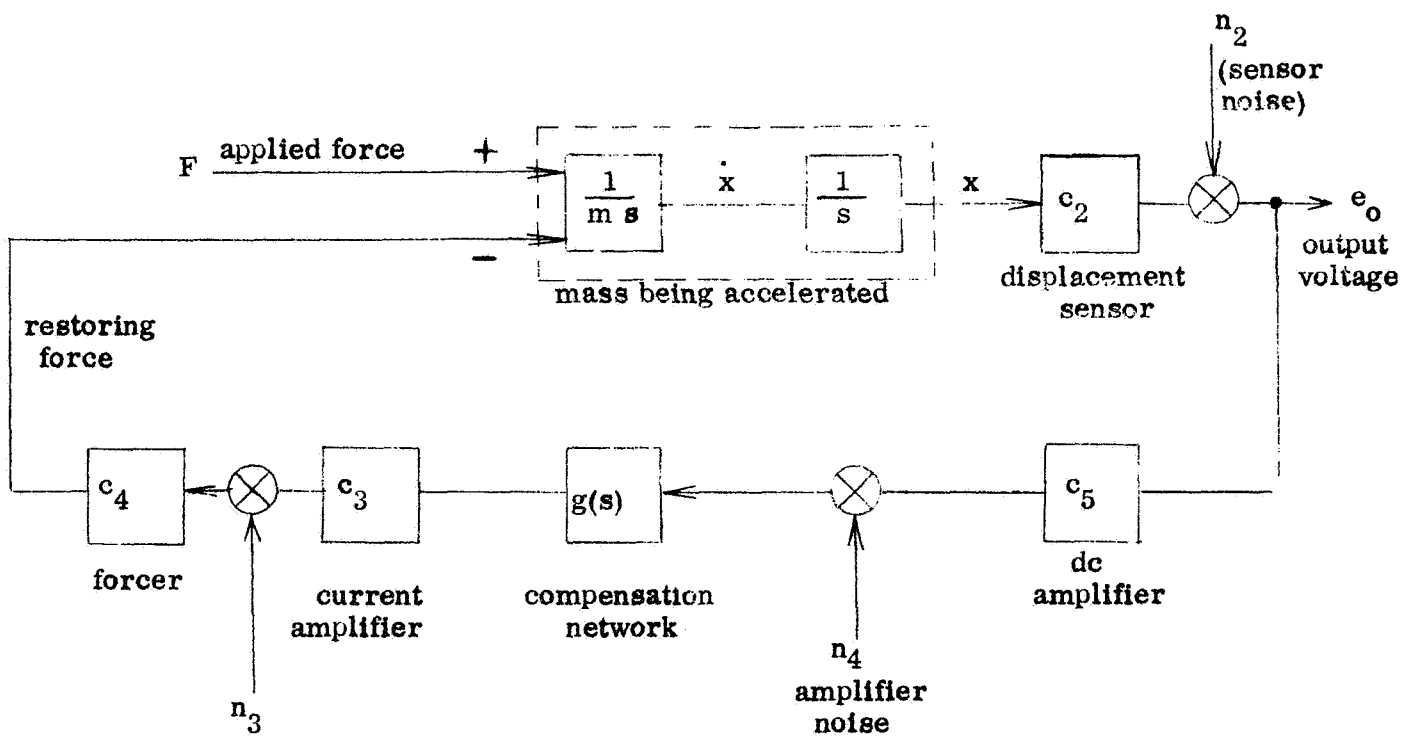
$$\alpha = \Omega / \sqrt{10}, \quad \beta = \Omega \sqrt{10}$$

and

$$n = C \Omega^2 = C_2 C_3 C_4 C_5 \beta / \alpha m$$

Adequate damping (60% of critical) with minimum gain is achieved if $C = 1.5$

and $\Omega / \Omega_o = 2.37$, $\Omega_o = 2\pi (250) \text{ rad/sec}$.



- c_2 displacement sensor (output) scale factor, volts/ft
 c_5 dc amplifier gain volts/volt
 $g(s)$ Compensation network; $g(s) = \frac{\beta}{\alpha} \frac{(s + \alpha)}{(s + \beta)}$
 c_3 Current amplifier transconductance, amp/volt
 c_4 Forcer scale factor lb/amp

Figure III-A-2: Block Diagram, System (2) - Electromagnetic Spring, Closed Loop, With Network Damping

The signal transfer function becomes:

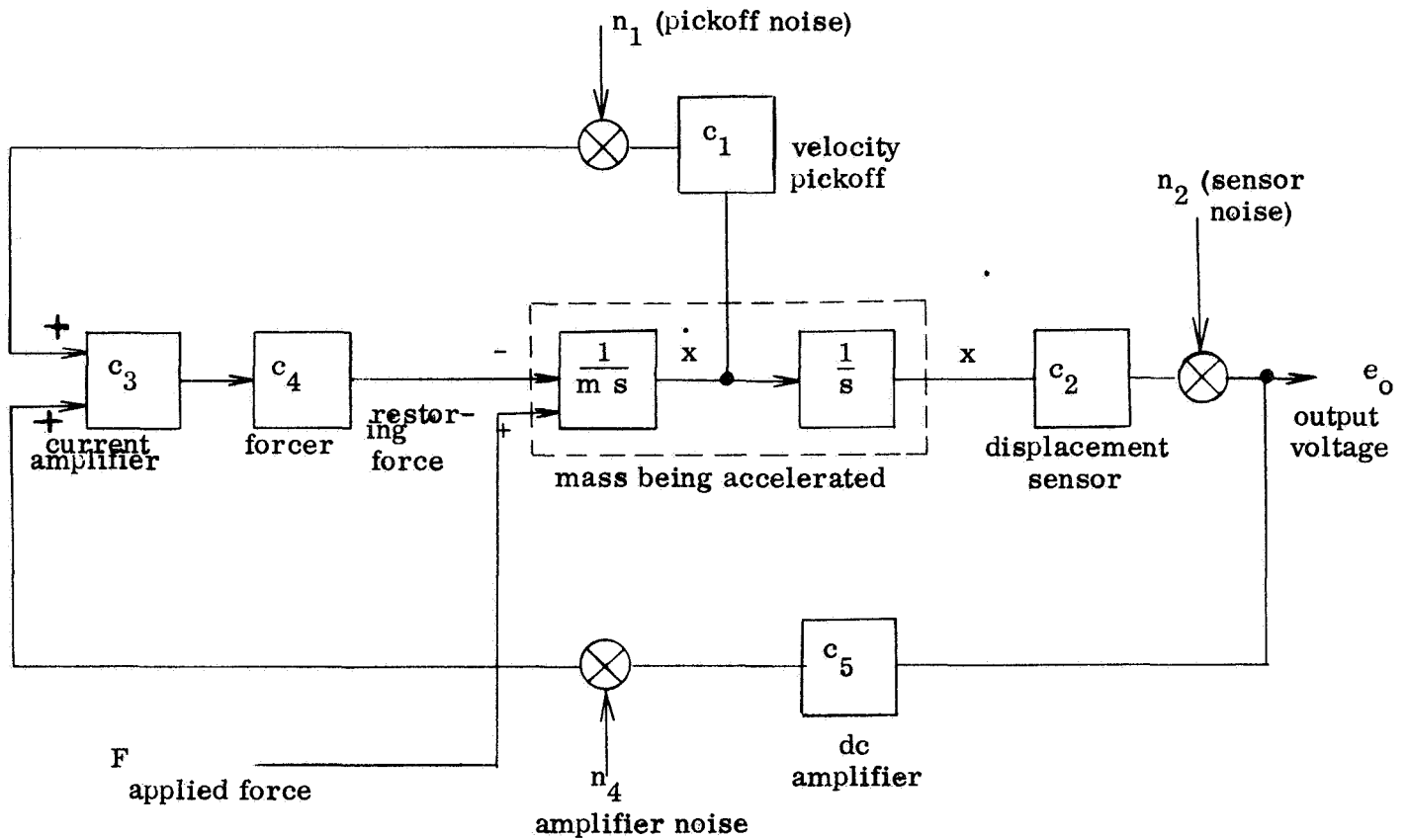
$$\frac{e_o}{F} = \left(\frac{C_2}{m} \right) \frac{s + 7.5 \Omega_o}{[s^2 + 1.174 \Omega_o s + \Omega_o^2] [s + 6.32 \Omega_o]}$$

Thus one concludes that

- a) The static calibration $e_o/F = 1/C_3 C_4 C_5$ volts/lb.
- b) The feedback loop (electromechanical spring) must be stable, well controlled, and all amplifiers must be D.C. amplifiers in order to provide steady state as well as dynamic stiffness.
- c) The sensor being the lowest level element, sensor noise N_2 is more difficult to control than noise at the other sources N_3 or N_4 . It is apparent that low frequency noise, N_2 , is greatly attenuated, which is a great advantage.
- d) The system is entirely insensitive to D.C. drift at the displacement sensor (the D.C. component of N_2) as the system corrects for such a noise output. Similarly, since this sensor is in the forward loop, the system is insensitive to hysteresis effects which might be present in the sensor.
- e) Noise levels at N_3 and N_4 must be kept low since they appear at the output like signal voltages.
- f) With a sensor operating at a suppressed carrier level the major contribution of gain may be achieved by A.C. gain, and the D.C. amplification will largely be one of providing isolation, current driving and impedance matching.

3. System 3 - Electromagnetic Spring, Closed Loop, with Electromagnetic Damping

As shown on Figure III-A-3 this scheme has an electromagnetic feedback loop to provide the equivalent spring stiffness, while damping is provided by electromagnetic forces proportional to the velocity. The system transfer function is



- c_2 High sensor (output) scale factor volts/ft
- c_5 DC Amplifier gain volts/volt
- c_1 Velocity pickoff scale factor volts/(ft/sec)
- c_3 Current amplifier transconductance amp/volt
- c_4 Forcer scale factor lb/amp

Figure III-A-3: Block Diagram, System (3) - Electromagnetic Spring, Closed Loop, With Derivative Damping

$$e_o = \frac{C_2 F - N_1 C_2 C_3 C_4 - N_4 C_2 C_3 C_4 + N_2 (ms^2 + C_1 C_3 C_4 s)}{ms^2 + C_1 C_3 C_4 s + C_2 C_3 C_4 C_5}$$

Pertinent system characteristics are:

- a) The displacement sensor D. C. drift does not appear at the output, but higher frequency noise at N_2 will be somewhat more prominent than in system (2).
- b) Noise voltages N_1 and N_4 will appear at the output in the same form as input forces.
- c) The loop gain, $C_2 C_3 C_4 C_5 / m$, must be set equal to $\Omega^2 = (1570)^2$ and C_1 must be adjusted to give good damping. Since there are two feedback loops the two adjustments may be made independently.
- d) The damping loop may use A. C. amplifiers.

In attempting to arrive at a conclusion as to the best system to employ it is seen that the selection of the sensor heavily affects the decision. A capacitive sensor can be designed to have either a high spring rate or a low spring rate depending on whether the system is to be open or closed loop respectively. A piezoelectric crystal on the other hand has such a high spring rate which is inherent in its construction that an electrical loop such as systems 2 or 3 is not practical.

Looking at the loops without regard to the type of pickoff, there are distinct advantages to the closed loop approach and system 2 is the most practical method. This system is insensitive to any displacement sensor D. C. drift or hysteresis and the low frequency noise sources are attenuated by $(2\pi f / \Omega_n)^2$. Further, there is no need for separate velocity sensing, thus simplifying the force transducer design.

B. DISPLACEMENT AND FORCE TRANSDUCERS

The foregoing discussions of closed or open loop systems and system responses presuppose the availability of transducers to meet the sensitivity requirements set by the frequencies and force values of interest. In fact this is one of the more difficult areas to satisfy, as the transducer parameters laid down in Section II show.

To ensure the best coverage of the system requirements, an industry survey was made of known manufacturers and users of thrust stands and force or motion transducers, the performance parameters of which covered similar areas to that of the required system.

The thrust systems or transducers produced by the following companies were investigated:

- 1) Hughes Research Laboratories, Malibu, California
- 2) Kistler Instruments Corp., Clarence, New York
- 3) Clevite Corporation, Cleveland, Ohio
- 4) Rocketdyne, Division of North American Aviation Corporation, Canoga Park, California
- 5) United Aircraft Corporation, East Hartford, Conn.
- 6) Minneapolis-Honeywell Regulator Co., Aeronautical Division, Minneapolis, Minnesota.
- 7) Republic Aviation Corporation

A short commentary is given on each of these systems, together with relevant information emanating from experience of their operation and on the applicability of any of the techniques to the present system.

1. Hughes Research Laboratories

This is a new system recently produced by the Research Laboratories of the Hughes Aircraft Corporation for use at NASA-Lewis Research Laboratories. As it is a new system, the users have had no experience of its operation at this time of writing.

The system is a "hard" stand with a design requirement calling for the stand natural frequency to be in excess of 100 cps with a 5 pound thruster package attached. The thrust range to be measured extends from 0.01 lb-force to 5.0 lb-force. The thruster package weight to be accommodated can extend up to 25 pounds with the consequent fall-off in natural frequency accepted. The unit incorporates a soft seismic type vibration isolation system to attenuate background vibration along

the thrust axis. The stand utilizes a closed loop system with the reacting force produced by a coil in a magnetic field. The transducer is a displacement-sensing linear variable differential transducer which has a sensing threshold in the order of 10^{-6} inch.

Differential transducers are susceptible to two temperature effects, sensitivity change due to resistance change and zero or null shift due to differential expansion between windings and slug. However, used in a closed loop system, as in this case, these two effects are compensated and cause no error.

A comparison of one parameter of the transducer used in this system to the requirements laid down in Section II indicates the limitation of this transducer for the present application. These figures indicate that a transducer sensitive to 10^{-9} inch displacement is required, whereas the LVDT transducer of the Hughes stand has a sensitivity of only 10^{-6} inch. The relevant factors from this system are that a closed loop system is used and vibration isolation is built-in; the differential transformer displacement sensor is entirely inadequate to meet the projected system requirements.

2. Kistler Instrument Corporation and Clevite Corporation

These two companies are represented in this report by piezoelectric transducers. No thrust stand of the parameters required is known to utilize the types of transducers that these companies produce. The discussions on the two companies' products are grouped here in one section as the same basic principle is utilized and the remarks on the performance parameters of the transducers are interconnected.

The piezoelectric transducers are dealt with in this section in some detail, since they are considered to be among the most practical means of detecting the small motions and forces involved in this system study.

The basic principle of piezoelectricity is well known, but it is less well known that it is produced in two different types of materials, that the side effects of these materials differ and that they can affect considerably the overall performance of the transducer.

Utilized as motion or force transducers, the piezoelectric materials are essentially charge producers when placed under stress. This effect is observed to be naturally present in some crystal materials, such as quartz, tourmaline or lithium sulphate, and can also be induced into some man-made ceramics, such as barium titanate or zirconate-titanate. Both types of material are very rigid and yet sensitive to extremely small motions, thus having the advantages of providing high frequency systems that are still sensitive to small forces. A typical transducer utilizing a quartz crystal element has a natural, unloaded frequency of 70 kc and is still sensitive to 0.002 pound force. A transducer sensitive to 0.0001 pound, as is required for this application, could be readily produced and still retain an unloaded frequency of approximately 15 kc.

The main detrimental aspect of both crystal and ceramic piezoelectric materials is the fact that they are A. C. generators. The generated charge produced within the material by an applied force leaks away across the element or through the read out circuit. The charge dissipation is generally a function of the first stage, or charge amplifier unit, of the detection circuit; although the dielectric resistivity of some materials can become limiting when the best charge amplifiers are utilized.

Additional side effects attendant upon most piezoelectric materials can also influence their performance as accurate transducers; the two main effects in this class being domain reorientation and pyroelectric effects (References 1, 2, 3 and 4). The magnitude of these effects depends very much upon the type of material utilized and the configuration of the piezoelectric element in the transducer.

The piezoelectric charge is produced by distorting the lattice arrangement of an asymmetric crystal. This distortion causes the displacement of an ion along an axis of the crystal lattice, giving rise to a dipole moment within the crystal. Within piezoelectric materials such as quartz, the dipole moments of this polarization effect sum across the plane of the material, producing an accumulated charge on the surface of the element. The axis of this polarization depends upon the direction of the stress and the direction of the crystal lattice orientation. The orientation of the crystal lattice for natural piezoelectric materials is established at the time of the formation of the crystal and is generally a fixed property. For such materials the effect of domain reorientation is not present.

For man-made polycrystalline materials, such as barium titanate, the reorientation process can be of marked importance. The direction of polarization in these materials is established by the temporary application of a voltage across the element. Although producing efficient charge generators, this method of fixing the domain orientation is relatively weak and over stressing or repeated stressing of these materials can cause loss of orientation in some crystals of the element, resulting in the lowering of the charge produced by any given stress.

The remaining important side effect is the pyroelectric effect, which is divided into the primary and secondary forms.

In the primary form, a homogeneous change in temperature of the element produces an accumulation of charge, similar to and indistinguishable from that produced by a mechanical stress. The secondary pyroelectric mechanism is that introduced by a temperature gradient, either in the piezoelectric element or in the element support structure, producing a mechanical strain in the element and so generating a charge.

In summary, piezoelectric materials can be said to be subject to three major sources of error:

- a) Charge dissipation, due to their own or the readout equipment resistivity.
- b) Domain reorientation, due to overstressing, or sometimes repeated shock stressing, causing a change in charge produced by any given stress.
- c) Primary and secondary pyroelectric effects. The primary effect is that in which a charge is accumulated solely by a homogeneous temperature change in the element. The secondary effect, that in which a charge is produced by differential expansion in the piezoelectric material or support structure.

Dealing with the two manufacturers considered in detail, Kistler and Clevite, more specific statements can be made about their transducers.

The Kistler units utilize quartz as the sensing element in the transducer unit. The use of this material removes one of the side effects, domain reorientation, as it is not subject to this effect. In fact, for the best operation, the quartz element is often highly prestressed, to obtain some "bias" in the crystal lattice distortion. Additionally, to compensate for the charge dissipation effect, the Kistler Company has developed charge amplifiers to a high degree; some units being available with an input impedance of 10^{14} ohms. This type of amplifier provides the ability for some force transducers to maintain a D. C. force indication to within 2% accuracy for as long as 20 seconds; the D. C. accuracy of the system diminishes exponentially with time. The quartz transducer is, however, still extremely temperature sensitive due to the pyroelectric effect and so still needs extremely careful thermal isolation or temperature control.

The Clevite Company utilizes piezoelectric ceramics in its transducer elements, usually barium titanate or lead titanate-zirconate. Like quartz, these materials suffer from charge dissipation, but they are also subject to domain reorientation and both pyroelectric effects. The Clevite Corporation, however, claims a new transducer configuration which virtually obviates all effects except charge dissipation. The configuration utilizes a ceramic element in a low stress shear mode, with the material polarization parallel to the load axis. It is claimed that this configuration has been successfully proven in an accelerometer application and could be utilized in a force transducer.

In summary, then, it can be said that the piezoelectric type transducer can provide high frequency, open loop systems that can be made sensitive to the millipound thrust levels specified. These transducers are largely A. C. units and will suffer from a continual charge dissipation drift in long term D. C. applications. In addition, they can suffer from errors caused by the side effects of domain reorientation and pyroelectricity, depending upon the material and configuration used. Thus, applied to the measurement of steady state, long term thrusts, these transducers have severe limitations. However, they could be applied to the measurement of pulsed thrustors, where the pulses are of less than 20 seconds duration for example and a definite zero thrust condition exists between pulses. For this application the transducer can be shorted each time the thrust passes through zero, ensuring that each pulse is measured from a known drift and temperature

compensated base line. This system would require that no thrust aberrations, caused by solenoid or valve operation on the thruster, would cause the transducer to approach zero charge while the package thrust pulse was on. Otherwise the shorting relay would operate and could produce large errors.

If these conditions are met, the application of certain piezoelectric transducers to pulse thrust measurements could be worthy of further investigation.

3. Rocketdyne, Division of North American Aircraft

This company has been responsible for the production of one low level thrust stand for one Air Force Department (ASD-Wright Patterson Field) and is presently engaged in the development of a high response transducer for another Air Force Department (Edwards Flight Test Center).

The first stand was produced approximately three years ago under a development contract. It is a "soft" stand (with a natural frequency of 1 or 2 cps) utilizing a capacitive transducer combined into a closed loop system with feedback force produced by an electromagnet.

This stand was designed as a general purpose unit to measure the steady state thrust of research and development items, particularly electric propulsion devices. In the higher thrust ranges it performed adequately, but at the low thrust levels, in the order of millipounds-force particularly of interest for electric propulsion and attitude control packages, the stand had inadequate sensitivity.

Attempts were made to improve the signal to noise ratio in the millipound range. These efforts were unsuccessful because, it is believed, the basic configuration of the capacitor sensor did not have the ability to resolve the stand's excursion in response to the low thrust levels. This stand is no longer used for the testing of thrusters in the performance range up to 100 millipounds thrust.

Rocketdyne is at present involved in the development of a high response thrust transducer. The sensing element of this was originally to be based upon a semiconductor strain gauge. This element has since been combined in series with a

accelerometer to better fulfill the requirements for this particular application. Discussion with Rocketdyne has brought forth the following points:

- a) The transducer is of very high response, having a natural frequency of about 11,000 cps.
- b) The response threshold is high compared to the thrust level for this Goddard application of 5 to 200 millipounds, the Rocketdyne range being initially set at 1/4 to 10 pounds.
- c) The transducer is temperature sensitive and required adequate heat sinks; it would require water cooling for long time applications in the presence of thermal loads.
- d) In the program under way, due to (c) and other considerations, the transducer is being developed as a short duration unit suitable for testing short time rocket firings.

4. United Aircraft Research Laboratories

The thrust stand developed by this group was produced for their own use in testing an electric propulsion device of steady thrust characteristics (References 5 and 6).

The thrust system uses a capacitive transducer, which is perhaps the closest known to the unit proposed by Republic, but the system generally has some important differences.

The capacitor motion transducer is used in a hybrid system which utilizes a feedback nulling force unit assisted by a spring. The nulling force is produced by a unit which generates its effect from the electrostatic force of a voltage across the plates of a condenser.

The capacitor transducer acts in one arm of a microwave bridge, the unbalance of which is amplified to produce the null force.

In its final form the thrust stand has a natural frequency in the order of a hundred cycles per second and is utilized to measure steady thrusts of a few millipounds, indicating that the capacitor unit has motion discrimination at least approaching that laid down in Section II.

The United Aircraft system is, however, susceptible to thermal drift in its present configuration. To date this drift has not been corrected, so that the cause or causes of it can only be surmised.

One possible cause could be the design of the capacitor transducer, which is not a balanced design, being used in only one arm of the bridge. Other causes could be the differential growth of support structures, subjected to temperature gradients, loading the transducer with spurious forces, a factor that must be obviated in the basic design of the system. Discussion on this thermal drift and actions to be taken to nullify it are presented in the section on Republic's recommended thrust system.

5. Minneapolis-Honeywell Regulator Co.

This company produces an accelerometer sensitive to acceleration in the range of 50 g to 10^{-5} g (Reference 7). The main point of interest about this item is the apparent, or deduced, ability to discriminate displacement in the order of 10^{-9} inches.

The accelerometer is a pendulum, null balance type of unit with the displacement sensed by a differential transformer. The effective arm length of the pendulum is one inch and the angular stiffness of the unit is 0.05 milli-radians per g. This converts to a displacement of 5×10^{-5} /g at the end of the pendulum arm. It is deduced that in sensing 10^{-5} g the transformer would be discriminating 5×10^{-10} inches displacement, if the system is linear. In verbal discussion, the responsible project manager concurs with the deduction; with a reservation on the assumption of linearity. Additionally, in laboratory checks it would appear that a threshold of 10^{-7} g had been established for the unit, with the implication that a displacement of at least 10^{-11} inches was being detected. The stability of the unit was not good under these conditions, but it is considered a good threshold indication.

This unit therefore indicates the highest sensitivity of any differential transformer unit investigated to date. The company limits its claims solely to the acceleration performance of the unit and makes no claim as to the reality of its apparent displacement discrimination; this aspect has not been specifically checked. Utilizing this unit solely as a displacement sensor in a closed loop null balance system, (as it is similarly applied in its present acceleration configuration) would appear to be a method of achieving the required thrust stand performance that is worthy of further investigation.

6. Republic Aviation Corporation

Republic has been investigating the application of an existing sensitive pressure gauge to the function of a force or displacement transducer. A pressure gauge, manufactured by MKS Instruments, Burlington, Mass., has been suitably adapted into a direct force measuring configuration and the unit, with the existing readout equipment is illustrated in Figure III-B-1. The principle of the transducer is that of back-to-back capacitors whose out of balance is detected by means of an A.C. bridge circuit. The configuration of the capacitor and the bridge circuit are depicted in Figures III-B-2 and III-B-3.

Initial tests have been carried out on this adapted unit to determine sensitivity and linearity. The force restraint element, a diaphragm spring which is also the moving element of the back-to-back capacitors, was found to have a spring rate of 3000 lb/inch; this was obtained over the range of 0.04 to 1.0 pound force by means of weights and a dial gauge. Using the existing detection circuit the transducer was found to be sensitive to a 20 milligram force (4×10^{-5} lb-force approximately), for which load a 0.1 millivolt D.C. output was supplied by the detection circuit. The detection circuit consists of the A.C. bridge, a cathode follower, a four stage amplifier and a phase sensitive detector.

Based upon the assumption that the spring rate found for the diaphragm still holds at the very small loads, the 20 milligram force produces a deflection of 1.33×10^{-8} inches. In effect, therefore, the transducer and detector as tested have an output sensitivity of 75 microvolts/ 10^{-8} inches.

From Section II, the design parameters of the transducer require a threshold sensitivity of 3×10^{-9} inches; at which deflection the transducer system, as it now is, would produce 22 microvolts.

The output from the system, however, can be increased by a number of techniques. First, the original air gap of the capacitors can be reduced. At present the gap is 7×10^{-3} inches; this gap can be decreased to the order of 1×10^{-3} with little trouble. The excitation voltage, at present 6 volts, can be increased to 100 volts. The threshold voltage for 3×10^{-9} inches motion can therefore be brought to approximately 2.3 millivolts with little change to the existing system. With such output, the threshold could be deemed several times lower than 3×10^{-9} .

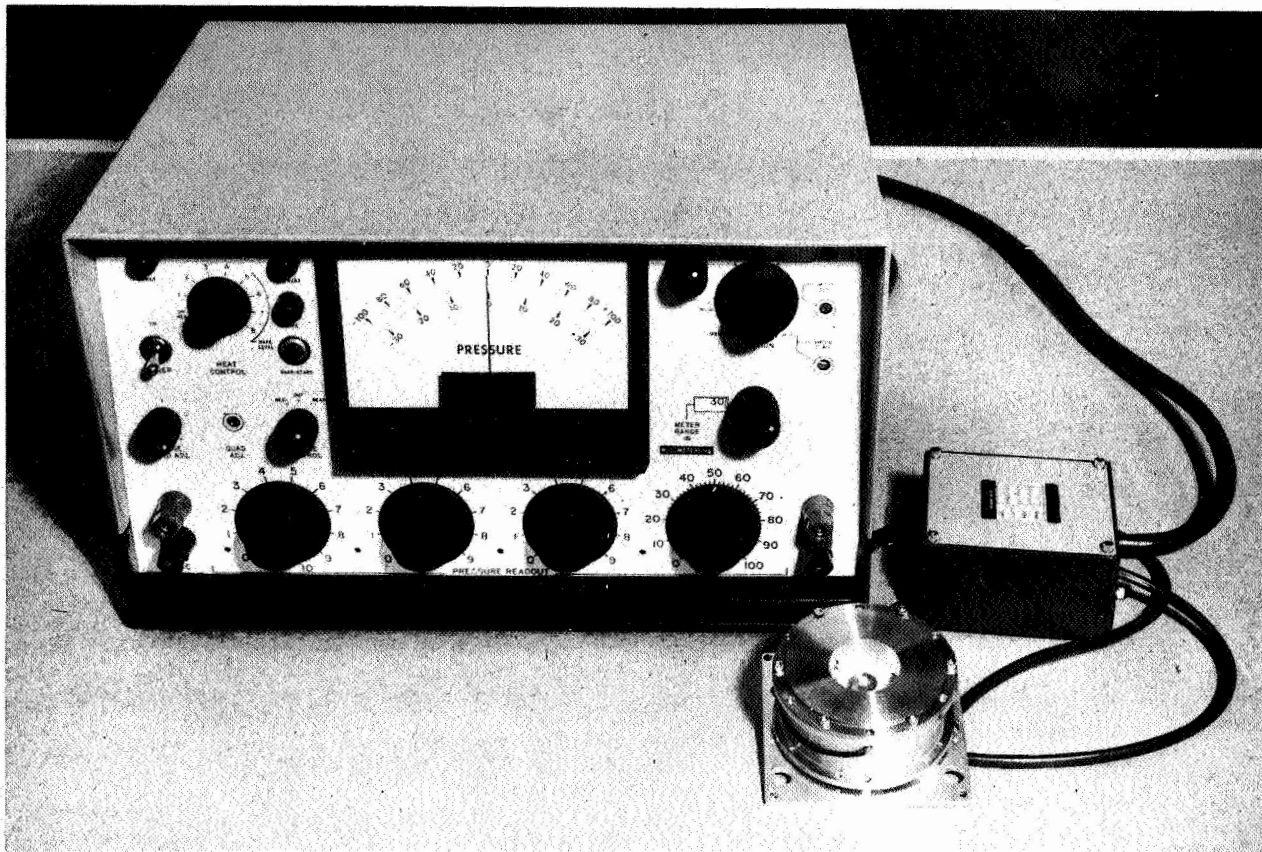


Figure III-B-1. Capacitor Transducer Equipment

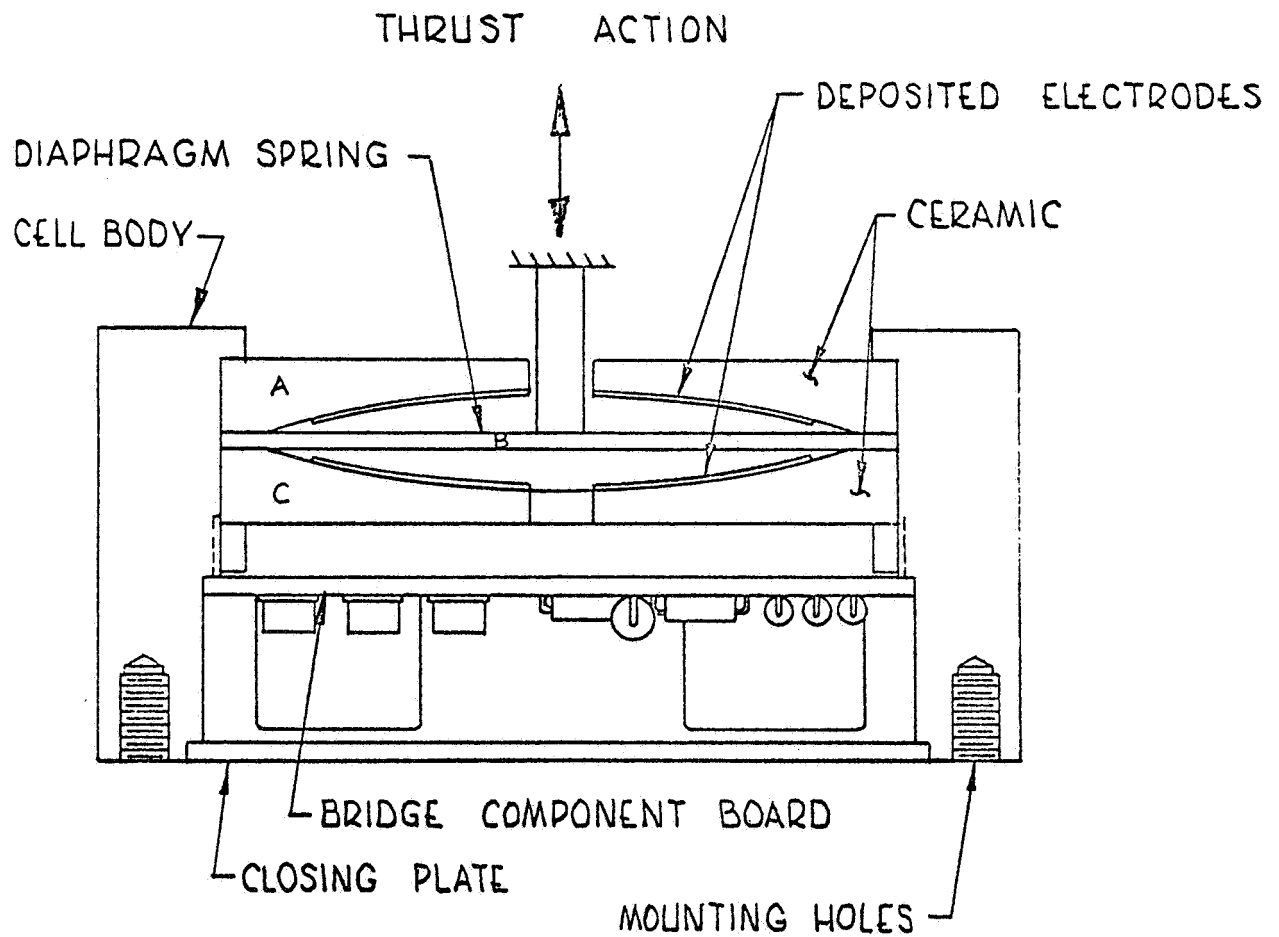


Figure III-B-2: Capacitor Transducer

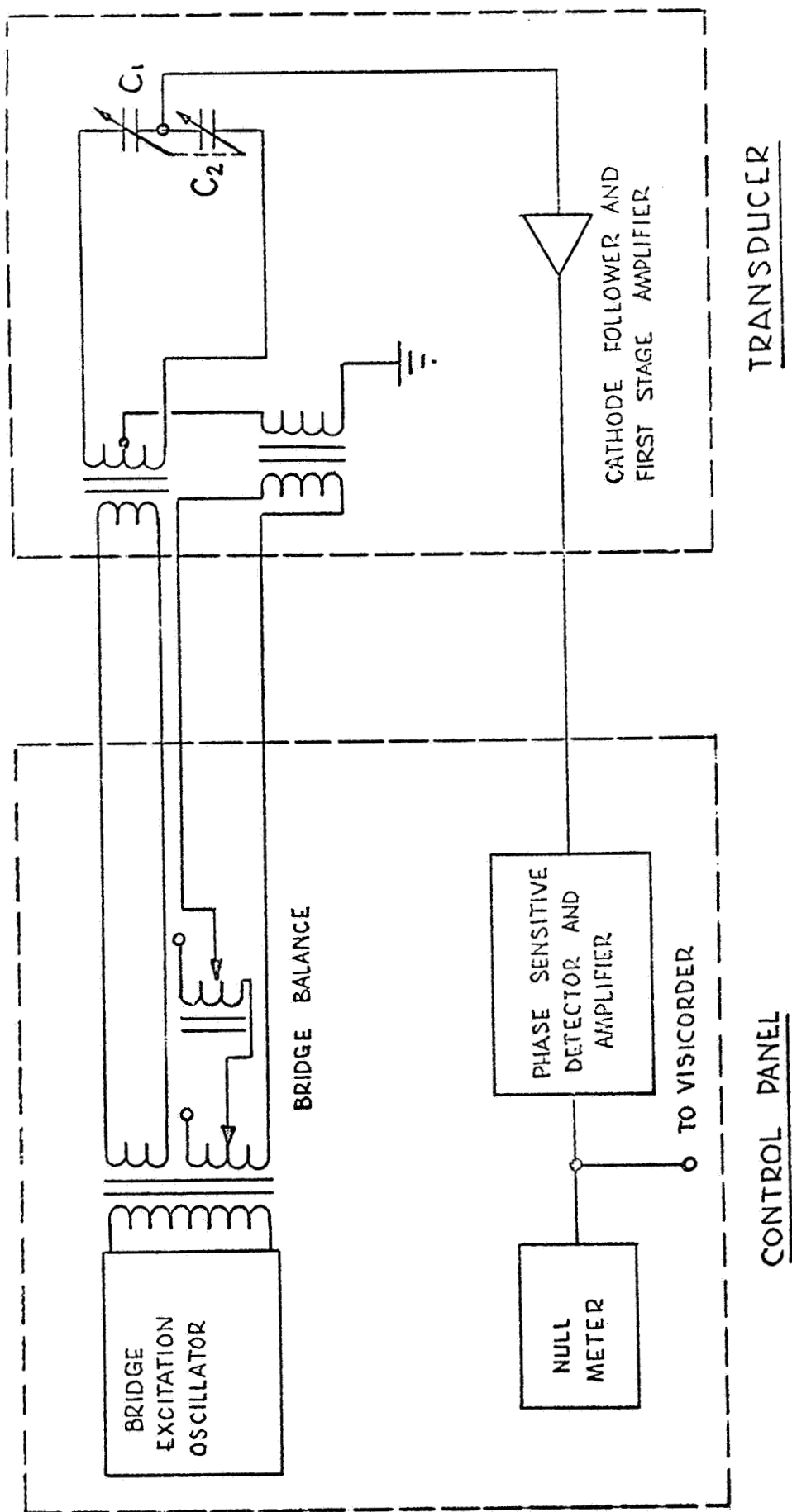


Figure III-B-3; Transducer Bridge Circuit

In obtaining this gain in output, care must be taken to avoid increase in system noise. Some improvement can be made in this aspect for the existing system: as thermionic tubes are used for the cathode follower and amplifier circuits, 60 cycle A.C. noise appears at the output. True D.C. voltage can be used for the cathode heaters to improve this aspect. Alternatively, since it is recommended that the thrust stand be initiated as a closed loop system, the transducer can be integrated directly into the loop system without recourse to its existing amplification circuit; the loop system being designed at the outset for low noise properties.

The capacitor transducer has been tested for linearity of output over the range 5 to 200 millipound and found to be adequately linear in this range, particularly as the proposed closed loop systems remove the necessity for much concern on this point.

Drift has been found to be present in the system during tests. As these tests were carried out in atmosphere it is possible that air currents were causing the small output variations that appeared in the 10^{-4} pound-force range. Until the loading tests can be carried out by remote operation in a closed chamber, this matter will not be resolved. Again, the closed loop system largely removes concern over this matter, so that the presence of this drift should not influence the choice of transducer.

Another factor having considerable influence on the transducer performance, temperature change, is well compensated for in the capacitor transducer. The two controlling capacitor elements in the bridge are constructed in intimate back-to-back configuration and additionally the transducer is temperature controlled at an elevated temperature close to 200°F.

In general it can be said that this transducer already has many of the attributes desired for the present application. The sensitivity of the unit is quantitatively known and it can be seen that this can readily be increased without improvements beyond present state-of-the-art.

C. VIBRATION ISOLATION

The thrust stand with its extremely sensitive, high bandpass, low force sensor will be subject to stray inertia forces produced by surrounding vibrations. These must be suppressed below the sensing threshold; this requires isolation of the sensitive part of the stand from the vibrating chamber.

The predominant interference is in the form of vibrations at 30 cps and of 0.32 ft/sec^2 (0.07 g) amplitude.

This section will present an analysis of the vibration isolation problem and indicate the design criteria for successful isolation. The thrust stand system is shown schematically in Figure III-C-1, where m_1 refers to the main thrust stand assembly and m_2 refers to the small thruster and moving parts of the sensing assembly. K_2 , C_2 refer to the stiff (250 cps) electromechanical thrust stand spring and damping, while K_1 , C_1 refer to the soft seismic suspension which acts as the vibration isolation. From this diagram

(mass m_1)

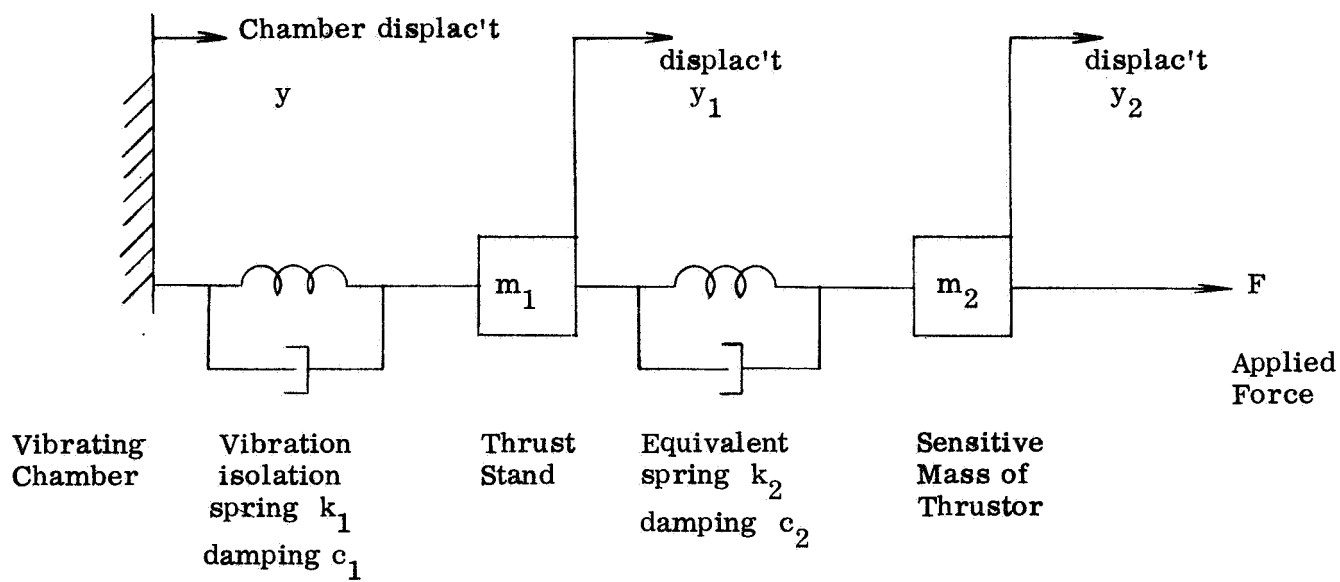
$$K_2(y_2 - y_1) + C_2(\dot{y}_2 - \dot{y}_1) - K_1(y_1 - y) - C_1(\dot{y}_1 - \dot{y}) = m_1 \ddot{y}_1 \quad (\text{C-1})$$

(mass m_2)

$$F - K_2(y_2 - y_1) - C_2(\dot{y}_2 - \dot{y}_1) = m_2 \ddot{y}_2 \quad (\text{C-2})$$

In these equations y is the chamber vibration amplitude, while y_1 and y_2 are the absolute displacements of the respective masses. Since the measuring instrument responds to the relative spring extension $x = y_2 - y_1$, these equations should be solved for the relative responses x/F and x/\dot{y} .

$$x = \frac{F(m_1 s^2 + C_1 s + K_1) - (C_1 s + K_1)m_2 s^2 y}{(m_1 s^2 + C_1 s + K_1)(m_2 s^2 + C_2 s + K_2) + m_2 s^2 (C_2 s + K_2)} \quad (\text{C-3})$$



y, y_1, y_2

absolute motions

$x = y_2 - y_1$

relative extension of sensor

Figure III-C-1 Vibration Isolation Schematic

This expression can be made more illuminating if one defines:

$K_2/M_2 = \Omega^2$ where $\Omega = 1570$ rad/sec, the cut-off frequency of the thrust measuring system.

$C_2/M_2 = 2\sigma\Omega$ where $\sigma = 0.6$, approximately, the relative damping of the measuring system.

$K_1/M_1 = b^2$ where b is the radian frequency of the seismic vibration absorber.

$C_1/M_1 = 2ab$ where a is the relative damping of the vibration absorber and $\mu = M_2/M_1$, the mass ratio.

Thus,

$$\frac{K_2 x}{F} = \frac{\Omega^2 (s^2 + 2abs + b^2)}{(s^2 + 2\sigma\Omega s + \Omega^2)(s^2 + 2abs + b^2) + \mu s^2 (\Omega^2 + 2\sigma\Omega s)} \quad (C-4)$$

$$= \frac{\left(1 + \frac{2as}{b} + \frac{s^2}{b^2}\right)}{\left[1 + \frac{2as}{b} + \frac{s^2(1+\mu)}{b^2}\right] \left[1 + \frac{2\sigma s}{\Omega} + \frac{s^2}{\Omega^2(1+\mu)}\right]} \quad (C-5)$$

$$\frac{\Omega^2 x}{\ddot{y}} = \frac{\Omega^2 (2abs + b^2)}{(s^2 + 2\sigma\Omega s + \Omega^2)(s^2 + 2abs + b^2) + \mu (2\sigma\Omega s + \Omega^2) s^2} \quad (C-6)$$

$$= \frac{1 + \frac{2as}{b}}{\left[1 + \frac{2as}{b} + \frac{s^2(1+\mu)}{b^2}\right] \left[1 + \frac{2\sigma s}{\Omega} + \frac{s^2}{\Omega^2(1+\mu)}\right]} \quad (C-7)$$

where the factoring of the denominator is an approximation valid if $b \ll \Omega$.

To obtain sufficient vibration isolation one should chose the vibration isolation frequency b such that the 0.01 g at 30 cps vibration produce no more relative displacement x than the minimum force bit of 0.10 millipound.

Since

$$\frac{b}{2\pi} \ll 30 \text{ cps} \ll \frac{\Omega}{2\pi}$$

one must satisfy

$$\frac{2ab}{(2\pi 30)(1 + \mu)\Omega^2} \ddot{y} \leq \frac{F_{\min}}{K_2} \quad (\text{C-8})$$

$$\frac{F_{\min}(2\pi 30)(1 + \mu)}{m_2 \ddot{y}} \geq 2ab \quad (\text{C-9})$$

$$\frac{2ab}{1 + \mu} \leq 0.38 \text{ rad/sec} \quad (\text{C-10})$$

Typically, $gm_1 = 200 \text{ lb}$ $gm_2 = 5 \text{ lb}$ $\mu = 2.5 \times 10^{-2}$ $a = 0.6$ (approximately)
Thus b must be chosen to be less than 0.32 rad/sec (0.05 cps), calling for a very soft seismic suspension. This suspension should of course be adequately damped ($0.5 < a < 1$). With such vibration isolation the effects of 30 cycle or higher frequency vibrations will be completely negligible. Note, however, that as a result of the introduction of this second mass/spring system there is some modification of the response due to thruster forces. Firdure III-C-2 shows asymptotic plots of the system frequency response with and without vibration isolation. Since $b \ll \Omega$ the distortion which occurs (due to the soft vibration isolator) is essentially of the form

$$\frac{1 + \frac{2as}{b} + \frac{s^2}{b^2}}{1 + \frac{2as}{b} + \frac{s^2(1 + \mu)}{b^2}} \quad (\text{C-11})$$

This is of course minimized if μ is small.

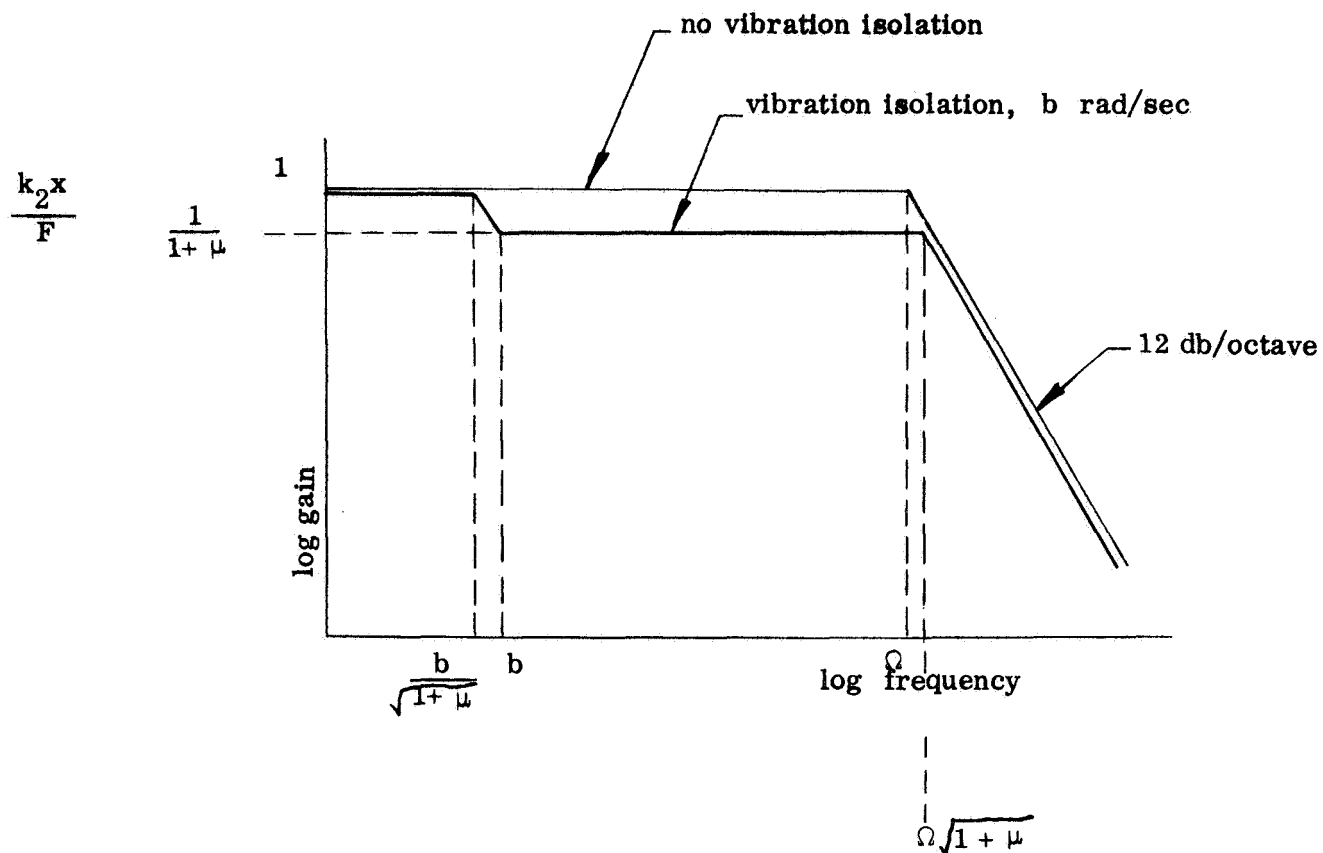


Figure III-C-2: Frequency Response Modification Due to Vibration Isolator

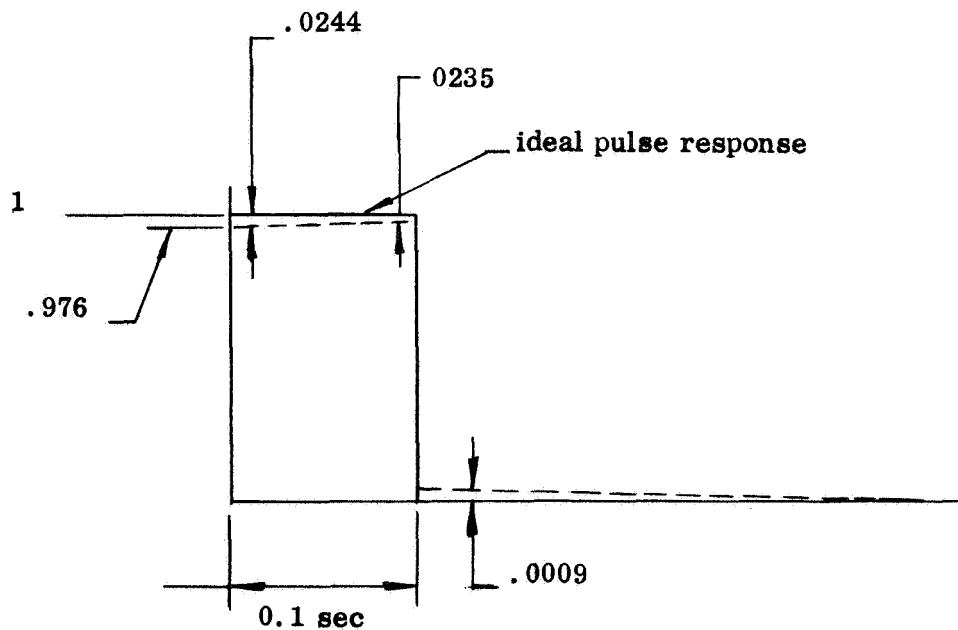


Figure III-C-3: Pulse Distortion

This is the reason for the design of a system having as small a sensing mass as possible with a large "isolating" mass. Figures of 5 pounds and 200 pounds have tentatively been chosen. For such a design the response to a step function input or impulse will suffer only very slight distortion. The step function response of the system will be

$$x(t) = 1 - \frac{\mu}{1+\mu} e^{-\beta t} \left(\cos \lambda t - \frac{\beta}{\lambda} \sin \lambda t \right) \quad (C-12)$$

where 1 represents the undistorted output and the remainder term is the distortion. In this expression,

$$\beta = ab/1 + \mu$$

and

$$\lambda = (b/1 + \mu) \sqrt{1 + \mu} a^2$$

Figure III-C-3 indicates (in an exaggerated fashion) the distortion of a 0.1-second pulse. While the pulse is present there is a 2.4% error. When the pulse is removed there is a small residual, amounting to less than 1/10 to 1% of the original pulse.

Since the output of the thrust stand is in the form of an electrical signal, it is possible to modify this signal through properly chosen networks to actually compensate for this 2.4% distortion. Thus if the system characteristics (μ , a , b) are known it is possible to design a network with characteristics reciprocal to equation (C-11). This correction is in effect a small additive correction as indicated by equation (C-13):

$$\begin{aligned} \frac{1}{F(s)} &= \frac{1 + \frac{2as}{b} + \frac{s^2(1+\mu)}{b^2}}{1 + \frac{2as}{b} + \frac{s^2}{b^2}} \\ &= 1 + \mu \left[\frac{\frac{s^2}{b^2}}{1 + \frac{2as}{b} + \frac{s^2}{b^2}} \right] = (1 + \mu) \left[1 - \frac{\mu \left(1 + \frac{2as}{b} \right)}{(1+\mu) \left(1 + \frac{2as}{b} + \frac{s^2}{b^2} \right)} \right] \quad (C-13) \end{aligned}$$

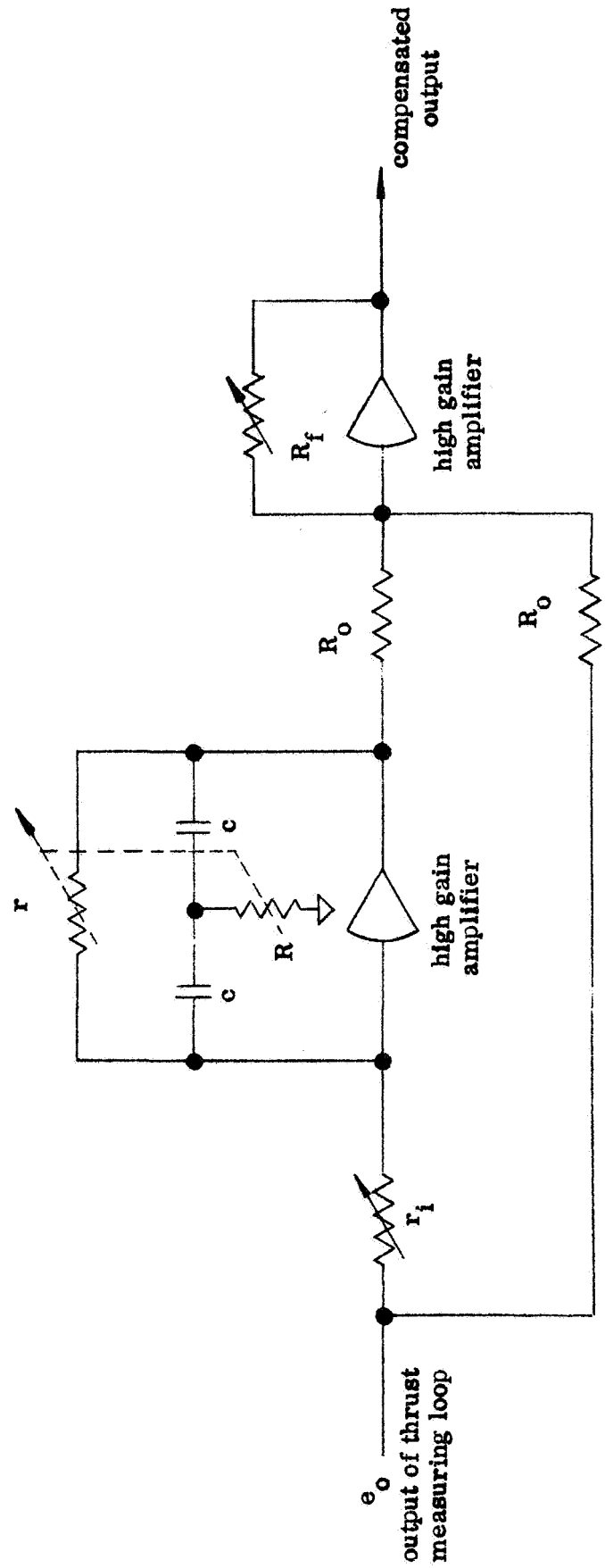


Figure III-C-4: Compensation Network

This may be readily realized with rather inexpensive computing feedback amplifiers, since the accuracy of the correction term is not too important. The 2.5% correction need not be more accurate than 5% of its own value.

Figure III-C-4 illustrates a method of accomplishing this; the transfer function of this compensating device being

$$\frac{R_f}{R_o} \left[1 - \frac{r}{r_i} \frac{(1 + 2RCs)}{(1 + 2RCs + rRC^2s^2)} \right]$$

which is of the same form as equation C-13. Adjustments are directly available to control

static gain ($1 + \mu$) by adjusting R_f

correction network gain (μ) by adjusting r_i

damping (a) selecting $R/r = a^2 = 0.36$

frequency (b) by common adjustment of R and r .

D. THERMAL EXPANSION ERROR ANALYSIS

Differential thermal expansion is one of the major sources of drift problems in thrust stand designs. There are major and minor effects which must be analyzed for each design in view of the anticipated temperature environment and the specific materials selected. An analysis has been made to determine the errors introduced by such effects.

The 4 bar linkage suspension is shown in Figure III-D-1. Linkages A, B, C and D are prestressed linkages, a necessary step taken to reduce the hysteresis of the flexure pivots below the threshold level required.

The bar BC (original length $a = a_R + a_L$) expands due to heating by an amount Δ_L to the left of the sensor and Δ_R to the right of the sensor. As a result the

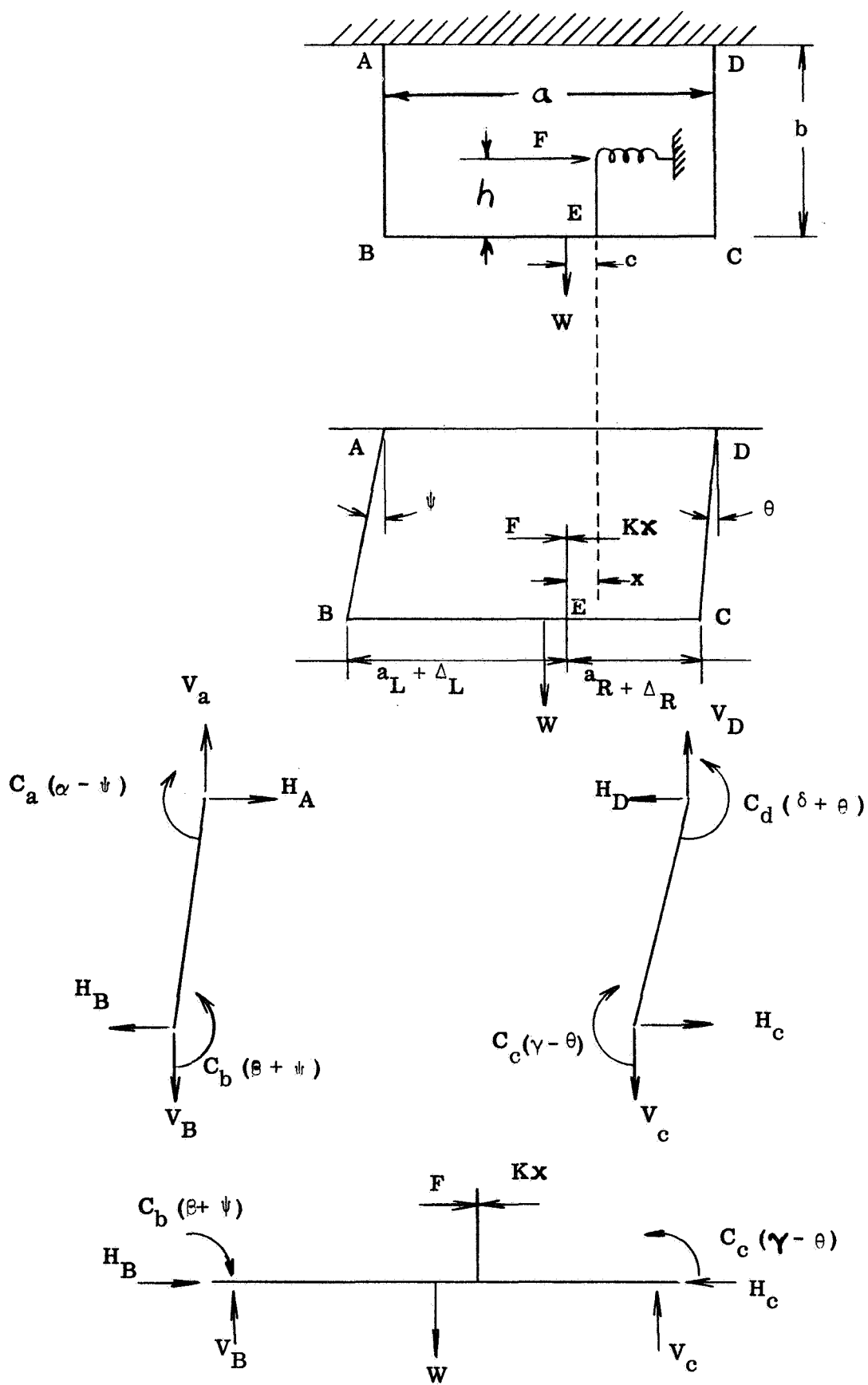


Figure III-D-1: Thermal Error Diagram

linkage bars AB, DC deflect through small angles ϕ, θ . Hence, the sensor displacement x which will be detected is

$$x = \Delta_L - b\phi = -\Delta_R - b\theta \quad (D-1)$$

From the free body diagrams one obtains

$$V_B + V_C = W \quad (D-2)$$

$$H_B - H_C = Kx - F \quad (D-3)$$

$$bH_B - b\phi V_B + C_a(\gamma - \phi) - C_b(\beta + \phi) = 0 \quad (D-4)$$

$$bH_C + b\theta V_C - C_C(\gamma - \theta) + C_d(\delta + \theta) = 0 \quad (D-5)$$

$$W(a_L + \Delta_L + C) + h(F - Kx) - V_C(a + \Delta_L + \Delta_R) + C_b(\beta + \phi) - C_C(\gamma - \theta) = 0 \quad (D-6)$$

In these equations,

K = main restoring spring constant (lbs/inch)

C_a, C_b, C_C, C_d = stiffness of the flexures (inch lbs/radian)

$\alpha, \beta, \gamma, \delta$ = flexure prestress angles (radians)

Solving these equations for the sensing element deflection x , one obtains (if second order terms are neglected)

$$\begin{aligned} x & \left\{ K + \frac{W}{b} + \frac{C_a + C_b + C_C + C_d}{b^2} + \frac{(\Delta_L + \Delta_R)}{a} \left[\left(1 - \frac{h}{b}\right)K + \frac{W}{b} + \frac{C_a + C_d}{b^2} \right] \right\} \\ & = F - \frac{C_a\gamma - C_b\beta + C_C\gamma - C_d\delta}{b} + \left(\frac{\Delta_R + \Delta_L}{a} \right) \left[\left(1 - \frac{h}{b}\right)F - \frac{C_a\gamma - C_d\delta}{b} \right] \\ & + \frac{W}{ab} \left[\Delta_L(a_R + C) - \Delta_R(a_L - C) \right] + \frac{1}{b^2} \left[(C_a + C_b)\Delta_L - (C_C + C_d)\Delta_R \right] \end{aligned} \quad (D-7)$$

Ideally one would like to see this relation to be

$$x K' = F \quad (D-8)$$

where K' is an equivalent spring constant; and in equation D-7 the predominant terms are of this form. The equivalent spring constant is

$$K + \frac{W}{b} + \frac{C_a + C_b + C_c + C_d}{b^2}$$

where K is much larger than the other terms.

The second part of the expression on the left side represents a small change in the effective spring due to temperature expansion; its effect is small. On the right side the significance of the various terms is:

F

the desired force

$$\frac{1}{b}(C_a \alpha - C_b \alpha + C_c \gamma - C_d \delta)$$

this represents a constant zero shift if the flexure preloads are not quite balanced.

This effect is corrected for by nulling the pickoff

$$\frac{\Delta_L + \Delta_R}{a} \left(1 - \frac{h}{b}\right) F$$

a term additive to the measured force, of order of magnitude less than $10^{-3} F$, thus, unimportant.

$$\frac{\Delta_L + \Delta_R}{ab} (C_a \alpha - C_d \delta)$$

a very small error if the flexures of A, D are unbalanced. It will be less than the required threshold.

$$\frac{W}{a b} \left[\Delta_L (a_R + C) - \Delta_R (a_L - C) \right]$$

this is the main source of error due to thermal expansion; it represents a fraction of the system weight appearing as part of the thrust. If unbalanced temperature

effects can exist ($\Delta_L \neq \Delta_R$) it is important that this term be kept below the system threshold. In order to minimize this error the thrust stand will be designed with a very large equivalent height b . This is achieved by the use of a seismic type support system as described later.

$$\frac{1}{b^2} \left[\Delta_L (C_a + C_b) - \Delta_R (C_C + C_d) \right]$$

This is a negligible unsymmetrical load; since it is divided by b^2 .

Equation D-7 permits detailed numerical evaluations of each of these effects to insure that no scale errors larger than 1/2% nor stray loads larger than 0.1 millipound are introduced.

E. CALIBRATION

The accuracy of the thrust measurement ultimately depends heavily upon the calibration techniques employed. The requirements for this high response thrust stand cover both a basic accuracy and an associated frequency response which implies that both static and dynamic calibration must be covered. The most direct means of providing static accuracy is through the use of an accurate weight acting through a variable moment arm, thereby applying a variable force to the thrust stand. This recommended approach has been used most successfully in the past and is capable of achieving an accuracy and resolution far better than that required for this thrust stand. The dynamic calibrator recommended is based on the static calibrator and correlates a D. C. current in an electromagnetic force element to the static calibrator. The current input may now be changed to an A. C. current, thereby establishing the overall dynamic response.

1. Static Calibration

Figure III-E-1 is a schematic of a steady state calibrator showing the placement of all major parts. A counter weight is moved along a balance arm by a screw thread, which is driven by an electric motor to provide remote operation. The load developed is applied, through a series of levers, to the mounting platform.

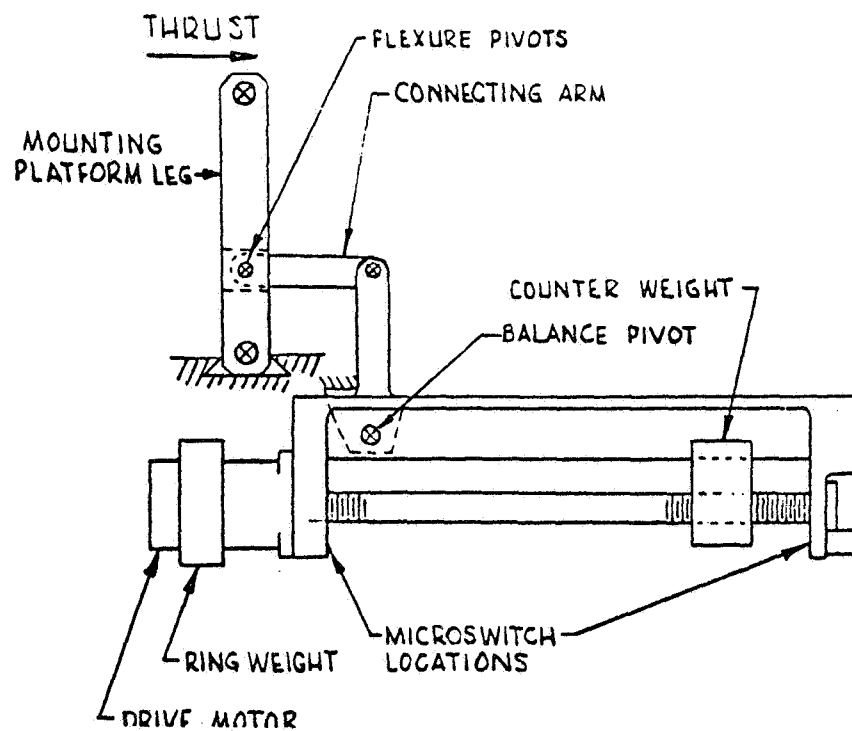


Figure III-E-1. Steady State Calibrator

The pivots throughout this mechanism are flexure pivots which eliminate friction and lost motion from the linkages. In addition their angular restraint is significant compared to that of the spring necessary to obtain a 250 cps response.

The calibrator is first balanced by use of the ring balancing weight, with the counterweight directly below the balance pivot. The maximum travel of the counterweight is governed by the placement of the microswitches which stop the drive motor. The inner microswitch is then positioned to cut off the motor whenever the counterweight returns to this zero position. Rotation of the screw thread then moves the counterweight away from the pivot, producing the calibrating load. Rotation of the screw is measured by an add-subtract counter, which receives six electric pulses per turn of the screw. Location of the weight is assessed from the number of pulses counted and the lead of the thread. The calibrator has various sources of error, all of them small.

Temperature effects

The various linkage arms can expand as a function of temperature. If all expand the same amount there will be no net effect. If the screw is hotter than the other linkages there will be an error. The coefficient of thermal expansion is 25 parts per million per degree F. A temperature difference of 200°F would therefore produce an error of only 0.5% of value. However, it is not expected that such a difference would in fact exist since this implies a very large heat source radiating only to the screw.

An even smaller problem is that relating to the angular preset of the pivots and the change in torque due to a change in temperature as described in the previous section, "Error Analysis." This is an order of magnitude less than the effect computed for the heavier pivots and is therefore not significant.

Weight Change Effects

Previous experience with outgassing of materials in a vacuum indicates that some care in the selection of materials must be given to guarantee that weight changes are small. It has been shown that aluminum can undergo a weight change of as much as 0.4 milligrams/in² when placed in a vacuum of 10⁻⁴ mm Hg. The surface area of the calibrator is about 30 in² and is centered about half way between the two end positions the movable weight may take. The weight change is

$$0.4 \times 30 = 12 \text{ milligrams}$$

and compared to the movable weight the error is

$$\% \text{ error} = \frac{12 \times 10^{-3}}{20} \times \frac{1}{2} \times 100 = 0.31 \% \text{ error}$$

Other materials such as phenolics, teflon, however, can undergo weight changes of two and three orders of magnitude greater than metals. The conclusion is that the materials other than metals may be used as long as they constitute only a small percentage of the total mass of the calibrator. This will be the case in the design of the calibrator.

Hysteresis

The small hysteresis present in the flexure pivots is avoided by virtue of the initial preset angle of a few degrees. Since the total deflection of the calibrator is less than the preset, the null positions of the pivots are never encountered.

Another source is that of the relative motion of the weight with respect to the screw. The nut will tend to ride against the driving side of the screw. Tolerances are set such that the backlash is less than the smallest bit to be detected.

It can be seen, therefore, that the various sources of error in the steady state calibrator will be small and the accuracy will be within the resolution of 2% of the bottom of the measurement range of 5 millipounds.

2. Dynamic Calibrator

Dynamic calibrator will be accomplished by using the steady state calibrator, the force coil, a stable D. C. current source, and a stable oscillator and amplifier. See Figure III-E-2. The steady state calibrator is set to the level at which the thruster is expected to operate and the recorder and carrier amplifier are adjusted such that this thrust causes a large swing on the recorder paper. The sensitivity is now known in millipounds per division. The D. C. current source is now adjusted to obtain a null. Next the steady state calibrator is set back to its zero position. The oscillator is now set at a low frequency - approximately 10 cps and the amplitude adjusted to be equal to the D. C. level. The record will be as follows:

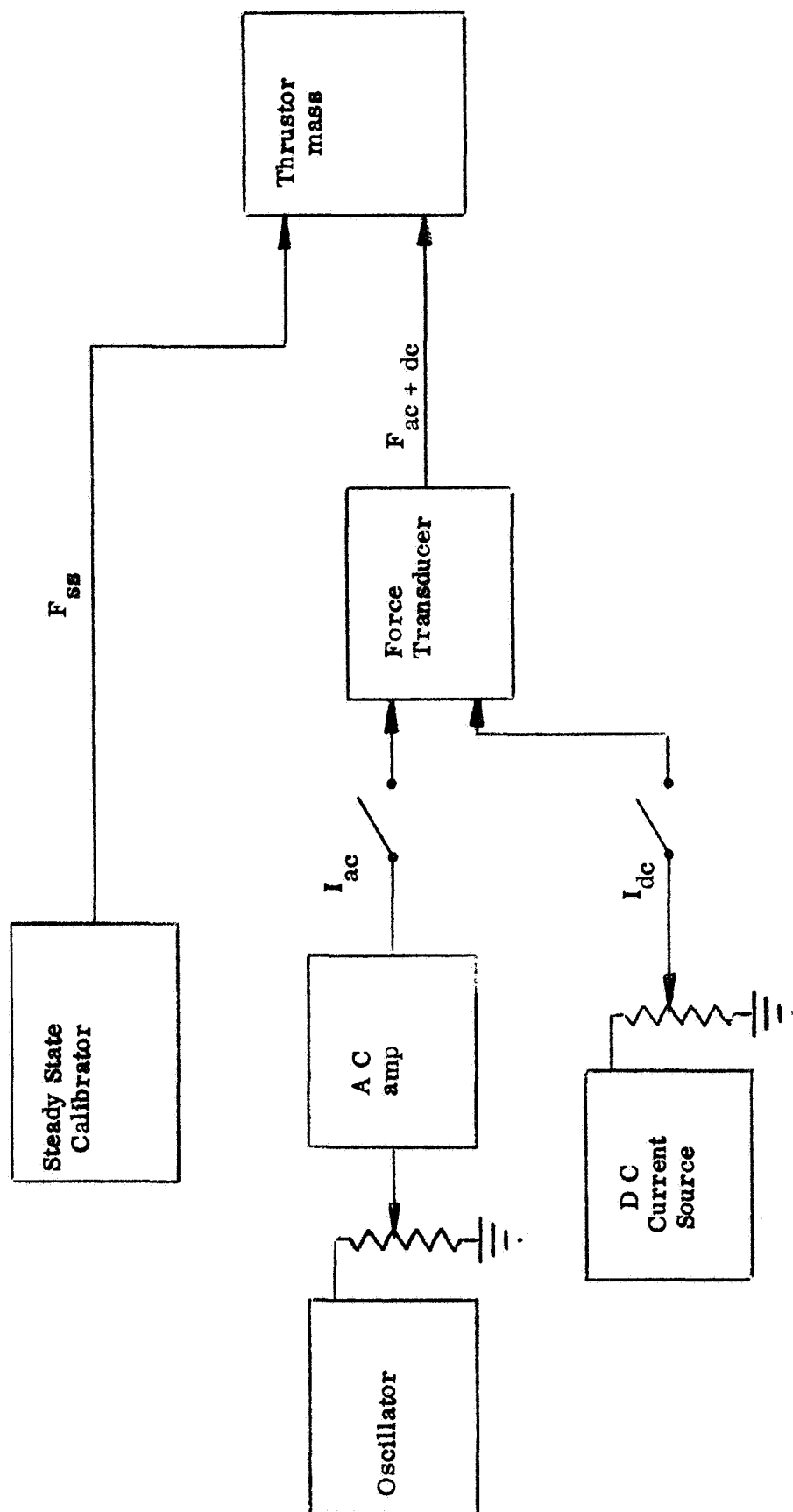
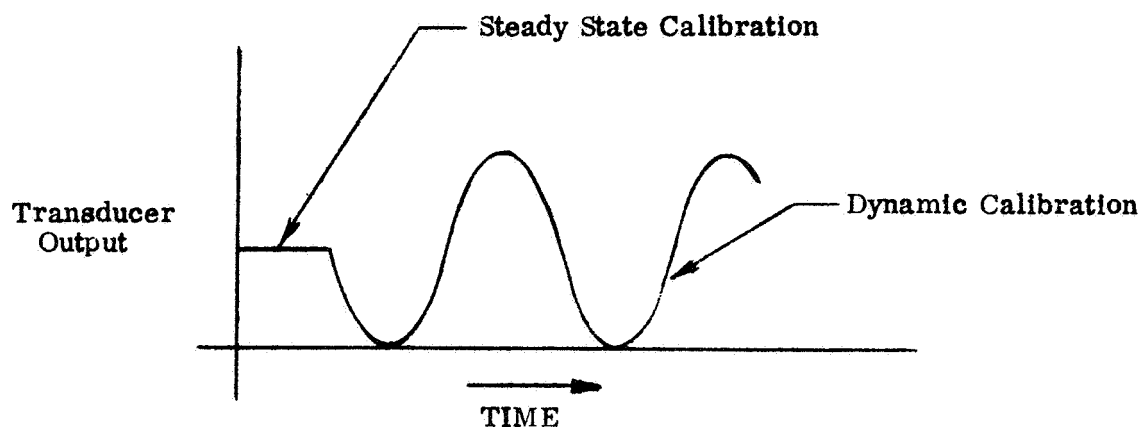


Figure III-E-2: Dynamic Calibration Sub-System



The A. C. signal must have a low harmonic content, be stable in amplitude, and have no D. C. component. Under these conditions the amplitude can be accurately set and the null point can be readily checked by removing both the D. C. and the A. C. input. The frequency may now be varied over the full spectrum and the response of the system recorded.

The question remains as to the linearity and dynamic response of the forcer elements before the response recorded can be concluded to be that of the loop alone. The forcer element described in Section IV is basically a speaker coil in a permanent magnet. Linearity can be demonstrated by comparing it to the steady state calibrator. Its dynamic characteristic can only be computed or be deduced by varying the mass on the table. This varies the natural frequency of the stand in a manner which should match the predicted values based on the mass change. The forcer element should not, however, produce any dynamic effects since it will be driven by a current source, thereby eliminating the effect of the inductance of the coil. In the frequency range of interest no other effect pertains. The field from the coil is two or more orders of magnitude less than the permanent field so that no hysteresis effects will be noted.

The amplifiers and current and voltage sources must be stable. This is obtained by selecting suitable equipment already designed to the proper specifications. Accuracy is not necessary for any of these elements as the overall accuracy is always referenced to the steady-state calibrator.

SECTION IV

THRUST STAND CONFIGURATION — RECOMMENDATIONS

Based upon the studies of the individual problem areas that have been covered in the foregoing sections, a general configuration of the thrust stand system has been arrived at and is now covered in this section. This system description is divided into the following special areas:

- . Vibration isolation
- . Test package support
- . Transducer location and mounting
- . Forcer motor
- . Calibrator
- . Supply lines and feed through
- . Control console

The proposed general configuration of the thrust stand proper is shown in the accompanying drawing No. PC 036D0000. A diagrammatic depiction of the effective suspension systems is shown in Figure IV-A-1. The operation of the thrust stand is described by reference to both the general arrangement drawing and the diagrammatic sketch.

A. VIBRATION ISOLATION

The test facility at Goddard Space Flight Center, into which the thrust stand is to be integrated, was studied in conjunction with a vibration mapping survey (Ref. 8), taken by Goddard personnel. The study and survey showed that a considerable amount of support equipment, such as vacuum pumps, liquid nitrogen cryostat, air compressor, etc., were intimately integrated into the test chamber's immediate surroundings. A considerable number of discrete background vibration frequencies, ranging from 25 cps up to 260 cps, were detected; with significant acceleration amplitudes (up to .05 zero-peak g)

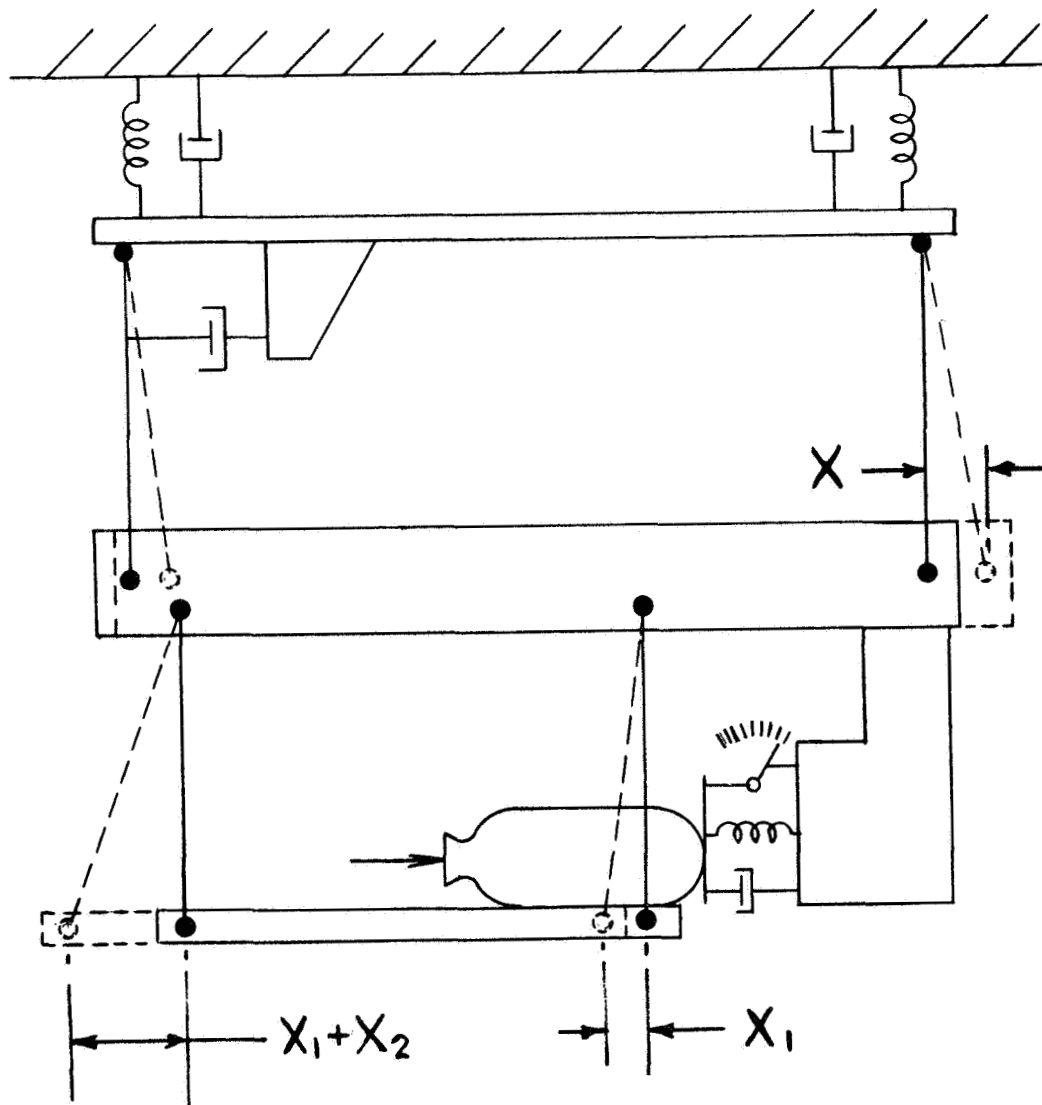


Figure IV-A-1: Thrust Stand Diagram

occurring at a number of the frequencies. The study made it apparent that it was highly impractical to attempt to isolate each of the vibration sources from the test chamber and, because of the chamber mounting and supply lines, equally impractical to isolate the chamber from the noise sources. The one practical method is to supply the hard stand with sufficiently soft mountings to attenuate the background noise to an acceptable value.

Although the lowest noise frequency was reported as 25 cps, other discrete frequencies were reported with one band appearing at 30 cps. Under these circumstances beat frequencies may occur at 5 cps.

To provide the best isolation, the thrust stand is designed with a very soft suspension (natural frequency $1/12$ cps approximately) in the direction of the thrust axis. As the diagrams in Figure IV-A-1 show, this is achieved by a pendulum suspension. The effective arm of this pendulum is made very long by the use of a seismic pendulum configuration as shown in the general arrangement.

The diagrammatic sketch also shows that isolation is provided in the two axes orthogonal to the thrust axis, so that cross talk of vibration from those axes into the thrust axis is attenuated. In the general arrangement these appear as special Lord vibration mounts. These mounts provide an isolation system with a natural frequency of 7 cps approximately. In addition, these mounts are so designed to maintain this natural frequency over wide variations of stand weight, so that the weight of the stand could vary from 200 to 400 pounds with virtually no change in the isolation. As reference to Analysis Section III-C shows, for good isolation in the thrust axis the mass mounted on the isolation pendulum should be 40 times the vibrating test package mass to maintain the thrust response of the system flat to within $2-1/2\%$ in the low frequency range. The mass of the isolated system should be approximately 300 pounds; the vibrator mounts providing, therefore, that considerable change

in system weight can be accommodated.

The diagram illustrates how the isolation pendulum deflects under the thrust load. Calculations show that, for a pendulum of 1/12 cps frequency a suspended mass of 250 pounds and a thrust of 200 millipound steady state, this deflection should be approximately 0.10 inches; a dimension well within the practical for the configuration.

B. TEST PACKAGE SUPPORT

It is necessary that the test package be supported so that its weight is removed from the transducer. Thus any weight change in the thruster is not reflected as a change of thrust. Also, the supporting method should contribute no spurious force input that may appear as thrust values. Some of these inputs could be caused by thermal growth of support structures or c.g. shift of the thruster due to its own temperature change. In addition, the mass of the support system that moves with the thruster must be low so that unnecessary loading of the system does not decrease the response frequency. Finally the structure must have high compliance to assist in maintaining the high response properties.

The method of support chosen is depicted in the diagram as a pendulum system. In fact, it is a seismic pendulum system with the angle of inclination close to zero, i. e. , at less than one-quarter degree. Under these circumstances the effective pendulum length for the configuration conceived approaches 2000 inches. It will be seen that this reduces the apparent thrust forces that temperature changes may produce.

The general arrangement drawing shows that two fixed water cooled walls are located to shield the stand from thermal radiation from the test package. However, to provide high response, intimate contact is required between the transducer and thruster and also between thruster and support. The transducer is effectively compensated against thermal

effects, as is described in another section. The immediate attachment of thruster to transducer will receive some heat load, as will the thruster mounting platform. The diagrammatic sketch, Figure IV-A-1, shows the effect of thermal growth at the transducer, which produces displacement x_1 . Thermal growth of the mounting platform produces a displacement x_2 at the other support, which adds to the x_1 also at this support point. If this displacement of the pendulum arm is large then, depending on the effective length of the pendulum and the portion of the thruster weight carried at that point, a significant apparent thrust force would be generated. It is intended that Invar or Nilvar material will be used at these two points. At the transducer attachment point the length of the Invar material will be 2 inches. Accepting a 200°F rise in this material and a coefficient of expansion 1×10^{-6} inch/inch/°F for Invar, the displacement

$$\begin{aligned} x_1 &= 2 \times 200 \times 1 \times 10^{-6} \\ &= 4 \times 10^{-4} \text{ inches} \end{aligned}$$

Assuming the whole thruster weight taken at this point, and the effective pendulum length of 2000 inches, the apparent thrust produced is

$$\begin{aligned} &5 \times 4 \times 10^{-4} / 2000 \\ &= 1 \times 10^{-6} \text{ lb/force.} \end{aligned}$$

A figure much below the required threshold of the system.

For the other support point, assuming a platform length of 10 inches

$$\begin{aligned} x_2 &= 10 \times 200 \times 1 \times 10^{-6} \\ &= 2 \times 10^{-3} \text{ inches.} \end{aligned}$$

and the apparent thrust would be

$$5 \times 2 \times 10^{-3} / 2000$$

$$= 5 \times 10^{-6} \text{ lb/force}$$

again, well below the threshold figure.

An additional load may be produced by the support platform due to the use of flexure pivots at the pendulum pivot points. These pivots remove all friction forces and lost motion at the suspension but do possess a spring rate under angular deflection. The thermal displacement x_1 and x_2 will produce such deflection at the pivots and the effect of the pivot spring rate is not reduced by the seismic pendulum configuration as is the weight effect. The pivots to be used have a spring rate of 0.10 lb/radian and as four of these are used at each support arm, the effective rate is 0.4 lb/radian. The true pendulum arm length for this case is 5 inches, so that the apparent thrust contributed by the pivot deflection due to x_1 becomes

$$0.4 \times 4 \times 10^{-4} / 5^2$$

$$= 0.8 \times 10^{-5} \text{ lb/force.}$$

At the other support point the thrust contributed by x_1 and x_2 is

$$0.4 \times 2.4 \times 10^{-3} / 5^2$$

$$= 4 \times 10^{-5} \text{ lb/force}$$

The spurious thrusts contributed by the thermal growth of the thruster mounting platform and transducer attachment therefore total to less than 1×10^{-4} pound, the thrust threshold value of the system.

C. TRANSDUCER, LOCATION AND MOUNTING

The basic parameters required of the transducer, or pickoff, of the system have been stated in a previous section and the various types of units that can be expected to meet these requirements have also been fully discussed.

Until further proving tests are carried out, no definite choice of the transducer type can be made. For the purpose of the general configuration study it has been assumed that the capacitor pickoff applies, as more information comes to hand on this unit. However, reference to the general arrangement drawing shows that the transducer mounting is well able to accept alternative units.

The stand configuration shows the transducer intimately coupled to the test package and located in line with the thrust axis. This method is considered to give the least attenuation between thruster and transducer and will achieve the highest practical response from the components of the system. Maintaining the transducer on the thrust axis reduces couples produced between thruster and the restraint and so reduces resonance produced in the mounting structure.

The transducer mounting provides that the axis of that unit may be moved, in conjunction with the location of the test package, to accommodate changes in the thrust axis of various thrusters.

D. FORCER MOTOR (Or Force Transducer)

The transducer is designed as a linear element over a wide range of force and frequency to be used as the feedback driving element in the closed loop as well as part of the dynamic and static calibration. The transducer will be capable of providing a steady state force of 150% of maximum or 300 millipounds. It is patterned after a speaker coil type element which is the most efficient means of using both the total copper and the maximum magnetic field available. Figure IV-D-1 is a cross section of the design. The magnetic field is radial everywhere in the gap while the current is circumferential everywhere in the gap. There are in fact many combinations of parameters which will result in a good transducer design. The ones presented are therefore not rigidly defined, but do represent a practical design. In addition to the direct computation of parameters there are a number of considerations and assumptions which are listed below:

- 1) The motion of the coil will be so small as to result in no appreciable change in effective magnetic field strength.
- 2) In a magnet assembly of this type no more than half of the total flux of the magnet will go through the gap. The remainder is leakage and cannot contribute to the generation of force.
- 3) The coil design will be based on the requirements of the driving amplifier so as to obtain a current proportional to the voltage input to the amplifier and independent of the inductance of the coil.
- 4) The magnetic field strength should be as high as possible in order to minimize both the heat losses in the coil and the cross-magnetization effects which could lead to a non-linear condition.
- 5) The weight of the magnet assembly is of no significance. Only the coil must be kept to as low a value as possible.

The basic equation used is the following:

$$F = 8.85 \times 10^{-8} B l i \text{ lbs}$$

where

B is in lines per square inch

l is in inches

i is in amperes

The flux density is first estimated on the basis of a preliminary magnetic circuit, considering leakage, saturation flux in the soft iron pole pieces, and the ratio of the gap to the magnet length. A driving current is then selected consistent with a practical amplifier output stage. The result is that the length of copper can be computed from the above equation. Considering such factors

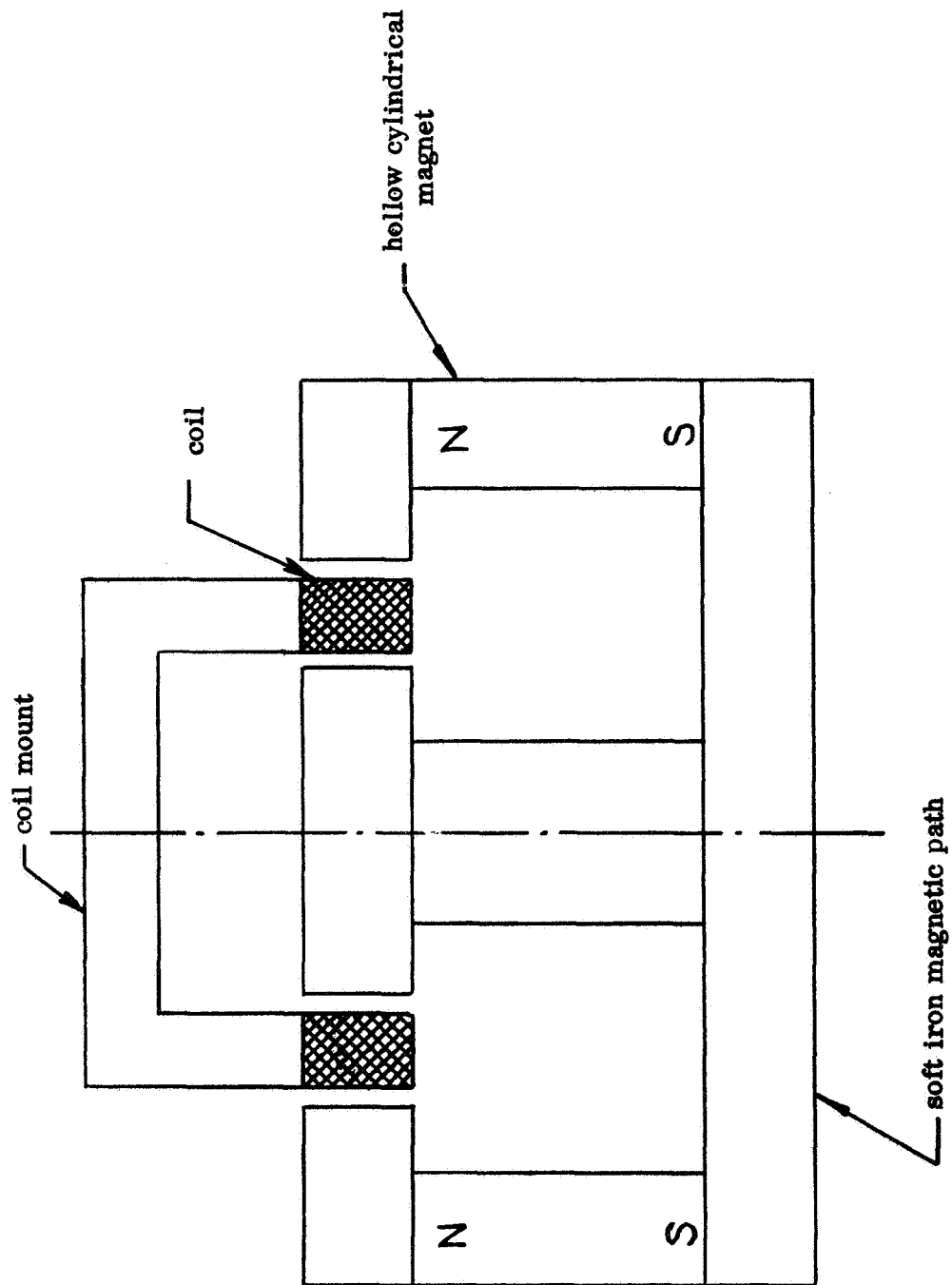


Figure IV-D-1: Forcer Motor

as the packing factor for round wire-layer wound, the clearance necessary and the assumed volume of the gap the maximum size wire is then selected. The dissipated power in the coil is the final item to be checked to assure reliable operation. At this point, any juggling of the current versus wire size with the gap volume fixed will only change the voltage level of the amplifier and coil but does not change the power dissipated. This can only be reduced by increasing the gap volume at the expense of an equivalent increase in magnet size and weight.

The preliminary design as presently conceived has the following specifications:

B_{gap}	=	25,000 lines per square inch
gap	=	0.25 lines
coil width	=	1.00
maximum current	=	20 ma
maximum force	=	300 mlb
wire size	=	#27
number of turns	=	1080
magnet	=	Alnico V
core material	=	Armco Ingot Iron
coil resistance	=	30
coil inductance	=	0.1 hy
magnet weight	=	2.7 lbs
magnetic assembly weight	=	10 lbs
maximum dissipated power	=	0.012 W

With the dissipated power so low, the magnet assembly could be reduced in size further. During the detail mechanical design of the stand this will be considered. In general it is desired to reduce the magnet as much as possible in order to reduce the amount of leakage flux external to the assembly. This flux will tend to exert a steady force on all iron or steel components within a

radius of about seven inches. As this force is essentially constant due to the extremely small excursions of the system under test it will only produce an offset which will be readily corrected for. In view of previous experience with a soft stand with large excursions it is not considered a problem.

This force transducer will be used as the driver element of the calibration subsystem as well as part of the feedback element of the closed loop. Further, it can also accept the damping signal. This mixing of signals may be achieved either at the input to an amplifier which drives the coil or by providing individual coils for each signal.

E. CALIBRATOR

As described in the preceding section, the force transducer for the closed loop system is also the driver unit for obtaining a dynamic calibration of the thrust stand. To provide a secondary force standard on the thrust stand, a steady calibrator is built into the thrust stand and is used as a reference for establishing the force of the dynamic calibration, as described in Section III E.

This steady state calibrator will be based upon the well proven design used previously on many of Republic's thrust stands. This steady state unit can in turn be checked against an NBS weight to establish the absolute performance of the system against a primary standard.

F. SUPPLY LINES AND FEED THROUGHES

It is anticipated that various forms of thrusters will be tested on the thrust stand and that for some of these it would be preferred that the fuel supply is located other than on the mounting platform. Two fuel lines will be provided to cross from the base of the thrust stand to the mounting platform and will be permanently attached. To ensure that these supply lines will not affect the thrust stand response a particular form of mounting, used successfully on a Republic soft stand, will be utilized. This configuration gives low resistance

to motion and yet water flow, at the rate of 8-1/2 lb/min at 30 psi, can be started and stopped and produce apparent thrust reaching below 10^{-4} pound. Fuel flow to low thrust packages should have no affect on the stand.

Electrical controls and instrumentation signals to and from the test package will be carried over the support pivot line by a flat conduction cable. Again these have been used successfully on previous stands and should prove more than satisfactory in this application.

It is anticipated that a 28 conductor unit will be provided. An additional unit can be readily added if required.

G. CONTROL CONSOLE

The console will be contained in a standard 19 inch rack unit. It will contain a series of separate racks carrying various control circuits of the system. Among the units will be a Type 1508 Honeywell Visicorder which will be used to provide a permanent record of calibration and thrust tests.

The console will contain the controls and readout facility for both the steady state and dynamic calibrators to provide remote operation of these units.

The circuits of the control loop of the system will be contained on racks to provide easy access for maintenance. Controls required for the adjustment of the loop such as gain damping, zero balance, quadrature balance, etc.; will be brought to the front of these racks.

SECTION V
REFERENCES

1. D. Berlincourt and H. H. Krueger, "Domain Processes in Lead Titanate Zirconate and Barium Titanate Ceramics," - Journal of Applied Physics, Vol 30, No. 11.
2. W R. Cook et al, "Thermal Expansion and Pyroelectricity in Lead Titanate Zirconate and Barium Titanate," - Journal of Applied Physics, Vol. 34, No. 5.
3. "Piezoelectric Crystal" and "Piezoelectricity," - Encyclopedia of Science and Technology, Vol. 10, McGraw-Hill Co., New York, 1961.
4. "Piezoelectricity" and "Pyroelectricity," - Encyclopedia of Chemistry, Rheinhold Pub. Co., New York, 1957.
5. "Investigation of an Oscillating Electron-Ion Engine for Space Applications," ASD Technical Documentory Report 62-410.
6. "Applied Research on an Oscillating Electron-Ion Engine," ASD Technical Documentory Report 63-253.
7. Minneapolis-Honeywell Regulator Company Aeronautical Division, Minneapolis, Minnesota Report No. U-ED 9939. Description of a low g accelerometer, No. GG 177B.
8. Memorandum: Mr. Charles Erath OTS to Mr. James Bridger OSS &SA, Vibration Survey of 4x5 Vacuum Chamber in Bldg 6 - Room S-7, NASA-Goddard Space Flight Center.

APPENDIX BANDWIDTH EXTENTION BY NETWORK COMPENSATION OR BY COMPUTATION

The thrust stand design discussed in this report has a "basic bandwidth" of 250 cps. This is defined as a linear system with second order response, adequately damped and with a corner frequency of 250 cps. It may be described as

$$F(s) = \frac{\Omega_o^2}{s^2 + 2\sigma\Omega_o s + \Omega_o^2} \quad (A-1)$$

where

$$\Omega_o = 2\pi (250) \text{ rad/sec}$$

$$0.5 < \sigma < 0.7$$

While such response speeds are considered quite fast for mechanical instrumentation systems, they nevertheless fall quite short in faithfully reproducing rapid pulses. For example, curve (A) of Figure A-1 shows a five millisecond square pulse. A system described by equation (A-1) would respond to such a pulse as in curve (B) of that figure. For comparison, curve (D) shows the response obtainable with a system which is ten times as fast ($\Omega = 2\pi (2500) \text{ rad/sec}$). Curve (A), Figure A-2 shows a more typical input for the thrust stand, an exponential pulse described by

$$\begin{aligned} i(t) &= \frac{1-e^{-Ct}}{1-e^{-1}} & t < \frac{1}{C} \\ i(t) &= e^{1-Ct} & t > \frac{1}{C} \end{aligned} \quad (A-2)$$

where $C = 200 \text{ rad/sec}$ $\frac{1}{C} = 5 \text{ milliseconds}$

Curve (B) shows the response of the 250 cps system; its predominant distortion is a lag of $\frac{2\sigma}{\Omega} = 0.765$ millisec. in following a ramp function input.

The question then arises whether it is possible to improve the performance of the basic system by judicious network compensation. As an alternative one might also attempt to compensate for the system distortion by computational techniques.

A first approach to a solution of this problem is to say that since the system distorts the input as $F(s)$ one should "undo" this damage by compensating by a function $F^{-1}(s)$ as indicated in Figure A-3. The compensation network is therefore

$$F^{-1}(s) = 1 + \frac{2\sigma s}{\Omega_0} + \frac{s^2}{\Omega_0^2} \quad (A-3)$$

Thus, one should take the output $h(t)$, and add to it its derivative and its second derivative, with the proper weighting factors $\frac{2\sigma}{\Omega_0}$ and $\frac{1}{\Omega_0^2}$ respectively. If this were done accurately (by step by step digital computation, or by analogue network simulation) one should reproduce the input precisely.

Further consideration indicates that this simple expedient is not a complete, practical answer to the problem. The direct application of equation (A-3) will greatly emphasize any noise $n(t)$ which might be present at the output. High frequency components of the noise (components at frequencies greater than Ω_0) will swamp any signal. Thus there is clearly an upper limit to the bandwidth extension. If a full description of the statistical properties of the input signal and noise were known then the conventional design theories, based upon the Wiener-Lee theory, would determine the optimum system configuration.*

*See for example, "Analytical Design of Linear Feedback Controls," by G. C. Newton, Jr., L. A. Gould and J. F. Kaiser - J. Wiley & Sons, 1957

Symbolically, if this optimized design technique led to a system design $\gamma(s)$, then one might decide to realize this system by building a "thruster stand" with characteristic $F(s)$ and a "compensator" with characteristic $\frac{\gamma(s)}{F(s)}$. If the noise were considerable then the "Compensator" might actually be a bandwidth limiting device instead of a bandwidth extension device.

For the design discussed in this report very little is known of the input noise characteristics. Internally generated noise (see Section III-A) can be minimized. Thus, it is assumed that some bandwidth extension can be realized before the amplified noise overrides the signal. The extent of this bandwidth broadening will of course be determined experimentally, by using variable bandwidth filters and measuring signal response errors and noise outputs.

It is apparent from the above considerations that the simple compensation (Equation A-3) is far from ideal, for two reasons:

- a) derivative networks are difficult to realize physically
- b) the indicated function is certain to amplify very high frequency noise to an intolerable degree

Thus, if signal and noise considerations were to permit a passband of $K\Omega_o$ (bandwidth extension by a factor of K) one should use "compensators" of the form

$$F_1(s) = \frac{1 + \frac{2\sigma s}{\Omega_o} + \frac{s^2}{\Omega_o^2}}{1 + \frac{2\sigma s}{K\Omega_o} + \frac{s^2}{K^2\Omega_o^2}} \quad (A-4)$$

or

$$F_2(s) = \frac{1 + \frac{2\sigma s}{\Omega_o} + \frac{s^2}{\Omega_o^2}}{\left[1 + \frac{2\sigma s}{K\Omega_o} + \frac{s^2}{K^2\Omega_o^2} \right]^2} \quad (A-5)$$

Figure A-4 shows the frequency response characteristics of:

$$F^{-1}(s) \quad \text{Equation A-3}$$

$$F_1(s) \quad \text{Equation A-4} \quad \text{and,}$$

$$F_2(s) \quad \text{Equation A-5}$$

Figure A-5 shows the resulting system responses $F(s) F^{-1}(s)$; $F(s) F_1(s)$; and $F(s) F_2(s)$ showing that the latter two extend the signal bandwidth by a useful factor of K without admitting extensive noise at frequencies much higher than $K \Omega_0$. If one wishes to perform this compensation by calculation rather than by analogue networks such cutoffs in frequency response are automatic. Thus one might tabulate the output at intervals of 0.20 milliseconds, and then difference these numbers twice to obtain the terms of equation (A-3). This choice of time interval automatically discards all frequency components in excess of 2.5 KC according to the sampling theorem $f_C = \frac{1}{2T}$.

Considering that the basic system function $F(s)$ has a gain of only 0.01 at $\omega = 10 \Omega_0$ it appears that bandwidth extension by more than $K=10$ is hardly practical since this would imply large gains of very small signals indistinguishable from noise.

A further consideration is the "identification problem". So far we have naively assumed that the system function $F(s)$ is known precisely. This is of course not quite true. After a system is designed its frequency response may be measured, gain and phase plots can be drawn and an analytic function fitted to describe $F(s)$. Experience with such measurements indicate that small nonlinearities result in a "band" of measured curves, and that furthermore there is not complete agreement in the characteristics derived from amplitude and phase measurements, respectively, as theory would indicate. Therefore, the numerical values for σ and Ω_0 in equation (A-1) cannot be precisely determined. Also, as derived in the equations on pages 10 and 12, there are other terms in the response which should be considered. The actual transfer

function is more nearly

$$\frac{(1 + \frac{s}{7.5 \Omega_o})}{(1 + \frac{s}{6.3 \Omega_o}) (1 + \frac{1.2s}{\Omega_o} + \frac{s^2}{\Omega_o^2})} \quad (A-6)$$

Other modifications to the transfer function become appreciable at higher frequencies due to mechanical compliances and amplifier cutoff.

Calculations were made to estimate the effects of these errors in estimating the parameters of a system transfer function.

Error in estimating system characteristic

Suppose the true transfer function is

$$F(s) = \frac{\Omega_o^2}{s^2 + 2\sigma \Omega_o s + \Omega_o^2} \quad (A-7)$$

and this is followed by a compensator

$$G(s) = \frac{s^2 + 2\sigma_1 \Omega_1 s + \Omega_1^2}{\Omega_1^2}$$

where Ω_1 is an estimate of Ω_o and σ_1 is an estimate of σ . If we apply a step input, then the output will reproduce the step plus an error

$$e_1(t) = e^{-\sigma \Omega_o t} \left\{ (\eta - 1) \cos \sqrt{1 - \sigma^2} \Omega_o t + \frac{1}{\sqrt{1 - \sigma^2}} \left(2\sigma_1 \frac{\Omega_o}{\Omega_1} - \sigma \eta - \sigma \right) \sin \sqrt{1 - \sigma^2} \Omega_o t \right\} \quad (A-8)$$

where $\eta = (\Omega_0 / \Omega_1)^2$

Curve (C) of Figure A-1 shows this response if both damping and frequency are estimated with 10% error; a similar computation was made for the exponential pulse and is shown in Figure A-2, curve (C). It is believed that actual estimation errors would be only about 5%.

To get a numerical measure of the "goodness of fit" the quantity

$$\varphi_1 = \int_0^{\infty} \epsilon_1^2(t) dt \quad (A-9)$$

was calculated and compared with

$$\varphi_2 = \int_0^{\infty} \epsilon_2^2(t) dt \quad (A-10)$$

where $\epsilon_2(t)$ is the error of an uncompensated system having K times the bandpass. In other words, $\epsilon_2(t)$ is the difference between input and output for a step input applied to

$$\frac{K^2 \Omega_0^2}{s^2 + 2\sigma K \Omega_0 + K^2 \Omega_0^2} \quad (A-11)$$

$$\epsilon_2(t) = e^{-K\sigma \Omega_0 t} \left[\cos \sqrt{1-\sigma^2} K \Omega_0 t + \frac{\sigma}{\sqrt{1-\sigma^2}} \sin \sqrt{1-\sigma^2} K \Omega_0 t \right] \quad (A-12)$$

The results are

$$\varphi_1 = \frac{(\sigma_1 \frac{\Omega_0}{\Omega_1} - \sigma)^2}{\sigma \Omega_0} + \frac{(\eta - 1)^2}{4 \sigma \Omega_0} \quad (A-13)$$

$$\varphi_2 = \frac{1}{2 K \Omega_0} \left(\frac{1}{2 \sigma} + 2 \sigma \right) \quad (\text{A-14})$$

Equating φ_1 and φ_2 one obtains a value of $K=15$ for 10% errors in σ and Ω_0 . This means that if one were to make errors of as much as 10% in estimating the system parameters the resulting mean square error of the compensated system would be equivalent to the mean square error of an uncompensated system with 15 times the original bandwidth! Clearly, the parameter estimation is no obstacle.

A further check was made, assuming that the actual transfer function is given by equation (A-6) but that an estimate of it neglected the two additional corner frequencies at $7.5 \Omega_0$ and at $6.3 \Omega_0$. Specifically, let $\epsilon_3(t)$ be the error if a step function $\frac{1}{s}$ is applied to

$$F_3(t) = \left[\left(\frac{\Omega_0^2}{s^2 + 2\sigma \Omega_0 s + \Omega_0^2} \right) \left(\frac{s+m}{s+n} \right) \frac{n}{m} \right] \left[\frac{s^2 + 2\sigma \Omega_0 s + \Omega_0^2}{\Omega_0^2} \right] \quad (\text{A-15})$$

and again $\epsilon_2(t)$ is the error of an extended bandwidth system (A-11).

$$\epsilon_3(t) = \left(\frac{n-m}{m} \right) e^{-nt} \quad (\text{A-16})$$

Again comparing errors on a mean square basis, namely,

$$\varphi_3 = \int_0^\infty \epsilon_3^2 dt = \varphi_2 = \int_0^\infty \epsilon_2^2 dt \quad (\text{A-17})$$

one obtains

$$\frac{1}{2n} \left(\frac{m-n}{m} \right)^2 = \frac{1 + 4\sigma^2}{4\sigma K \Omega} \quad (\text{A-18})$$

This indicates that the error in neglecting the two corners at $6.3 \Omega_0$ and $7.5 \Omega_0$ is equivalent to the error caused by a system with $K=500$ times the original bandwidth!

One concludes therefore that:

- a) if the noise level is low it is possible to extend the system bandwidth.
- b) for moderate widening ($K=5$ to 10) the system characteristics need not be ascertained more accurately than to within 5% to 10% which is not difficult. Higher order terms in the transfer function may be ignored.
- c) such compensation can be done in real time in the form of feedback amplifiers similar to the scheme of Figure III-C-4, or can be done in the form of digital computation subsequent to the gathering of data.

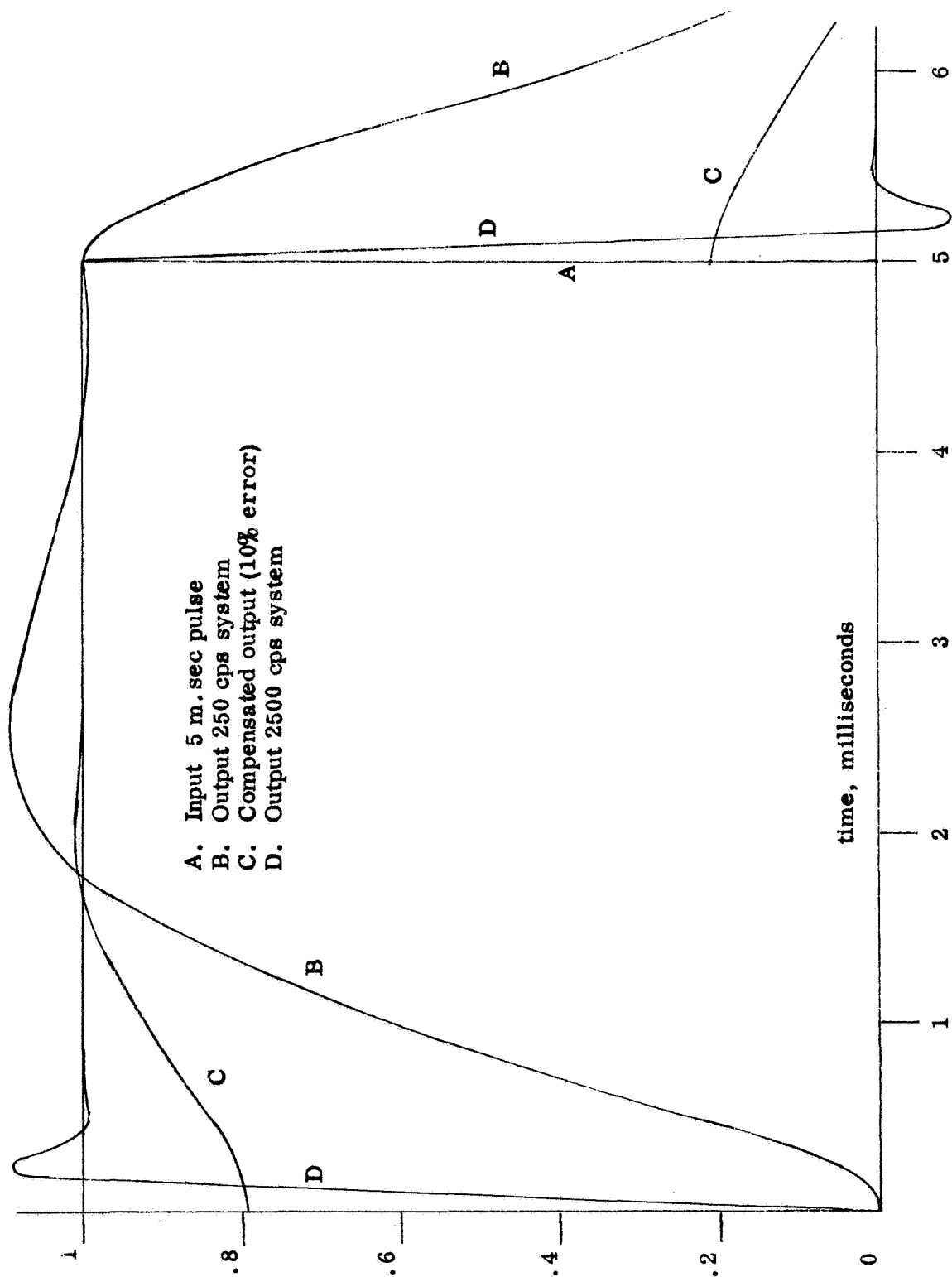


Figure A-3 Square Pulse Response

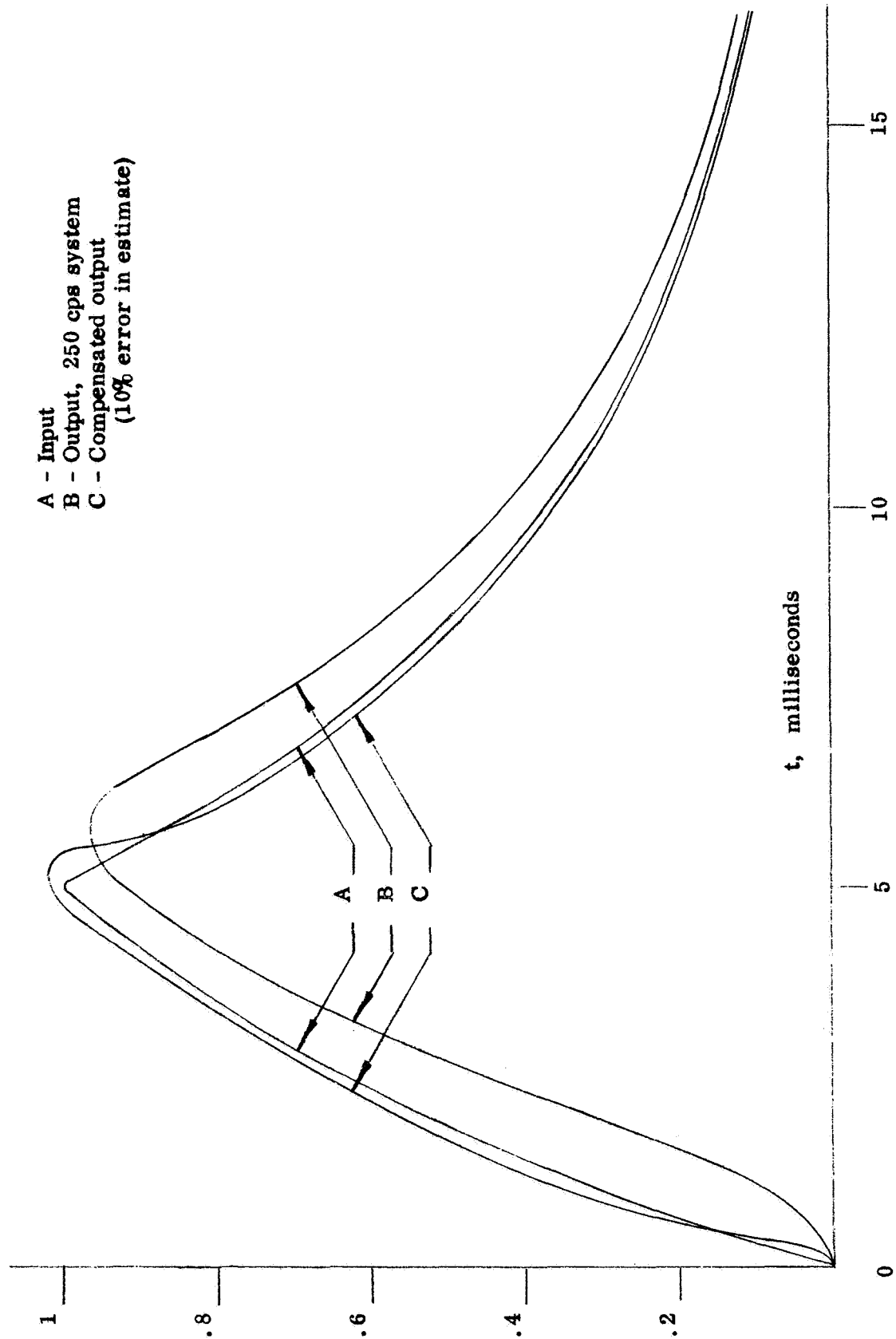


Figure A-2: Exponential Pulse

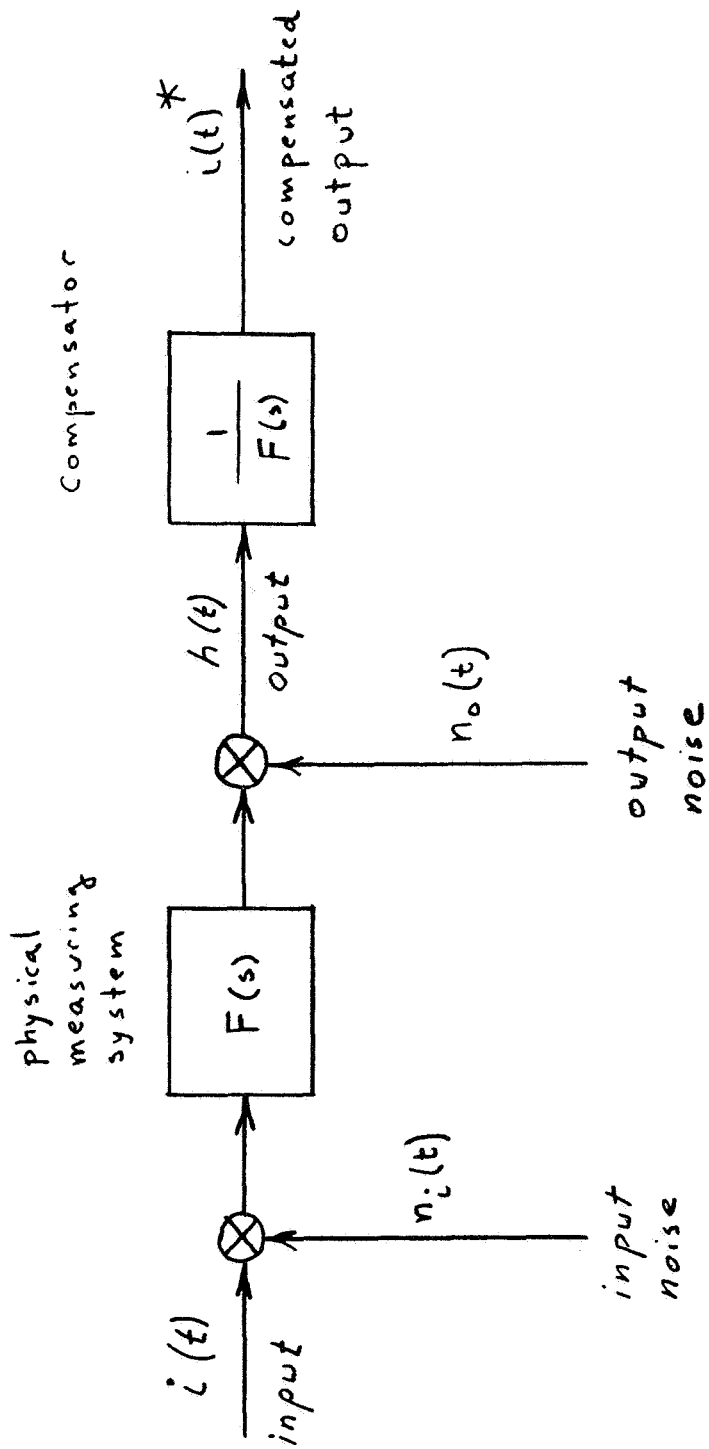


Fig. A-3

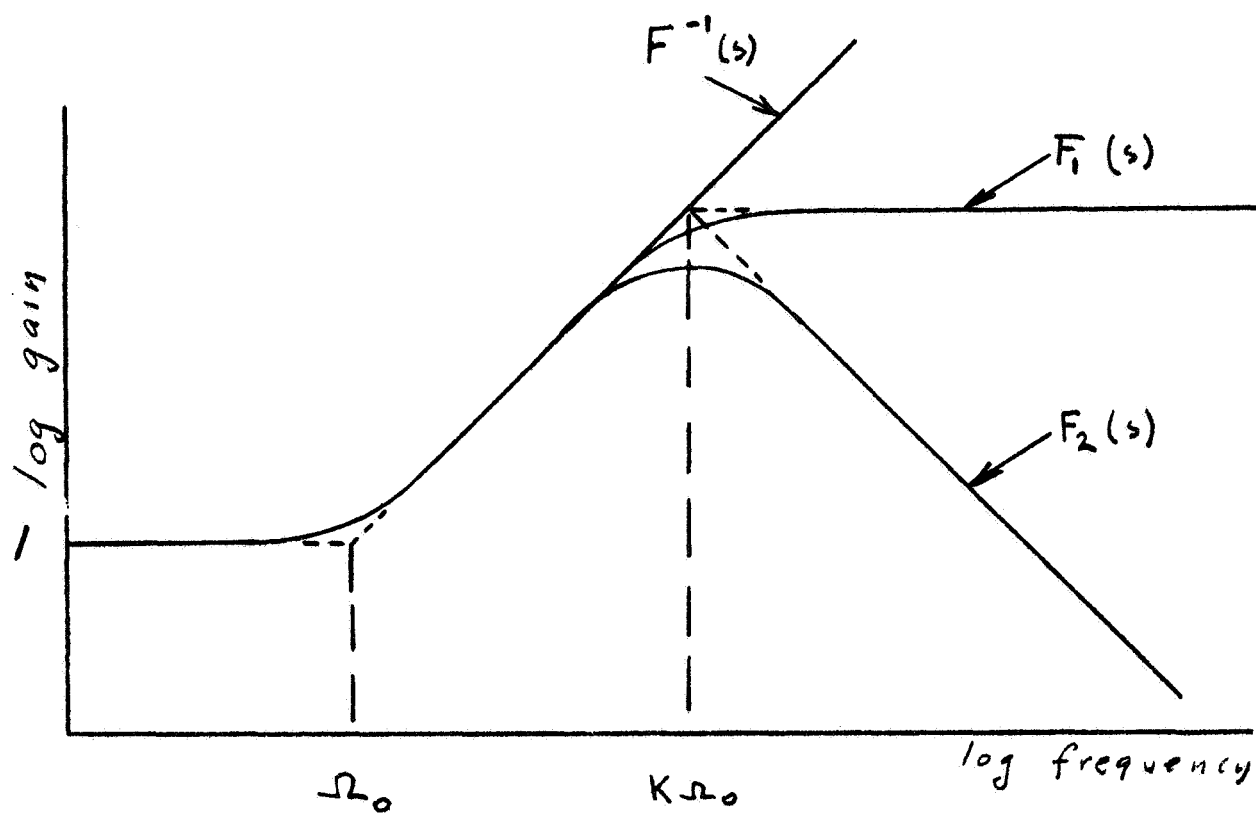


Fig A-4

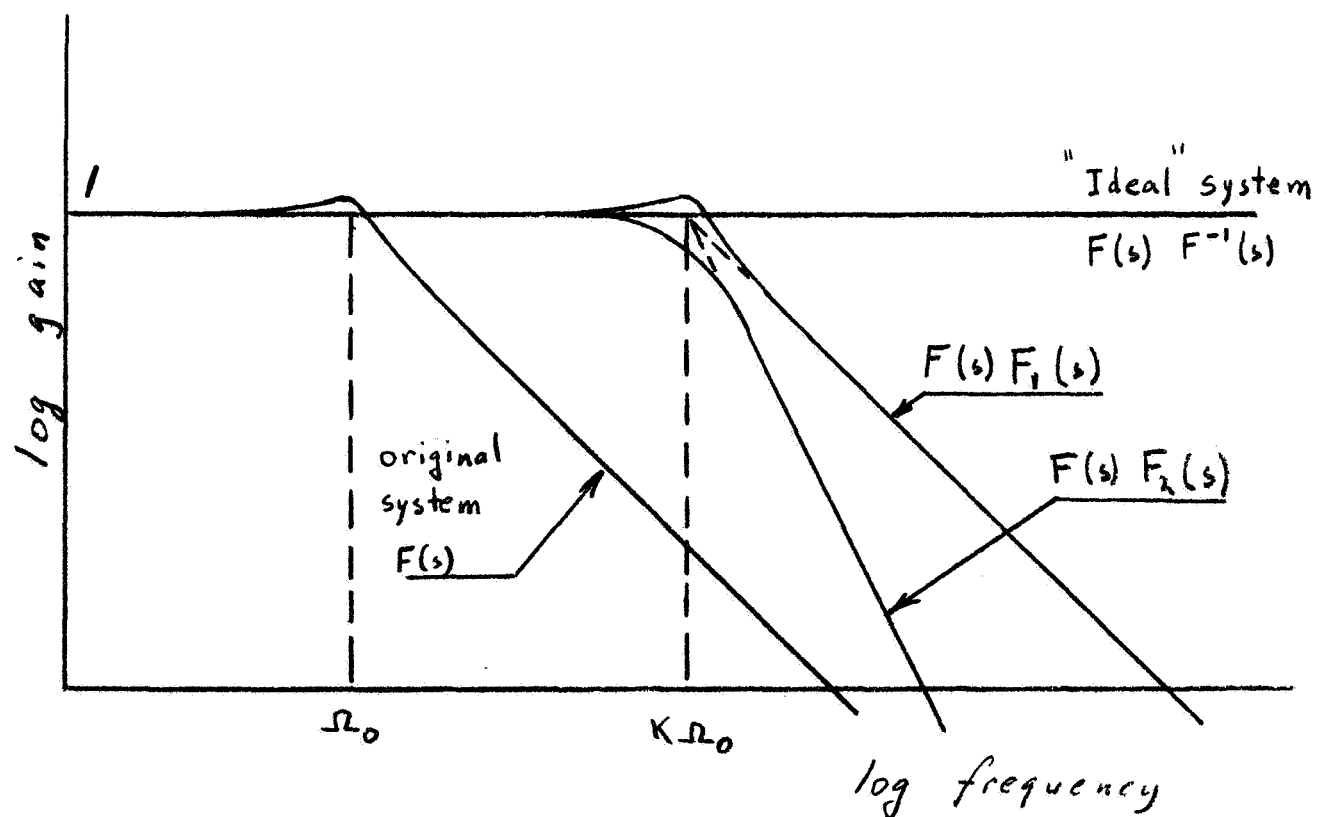
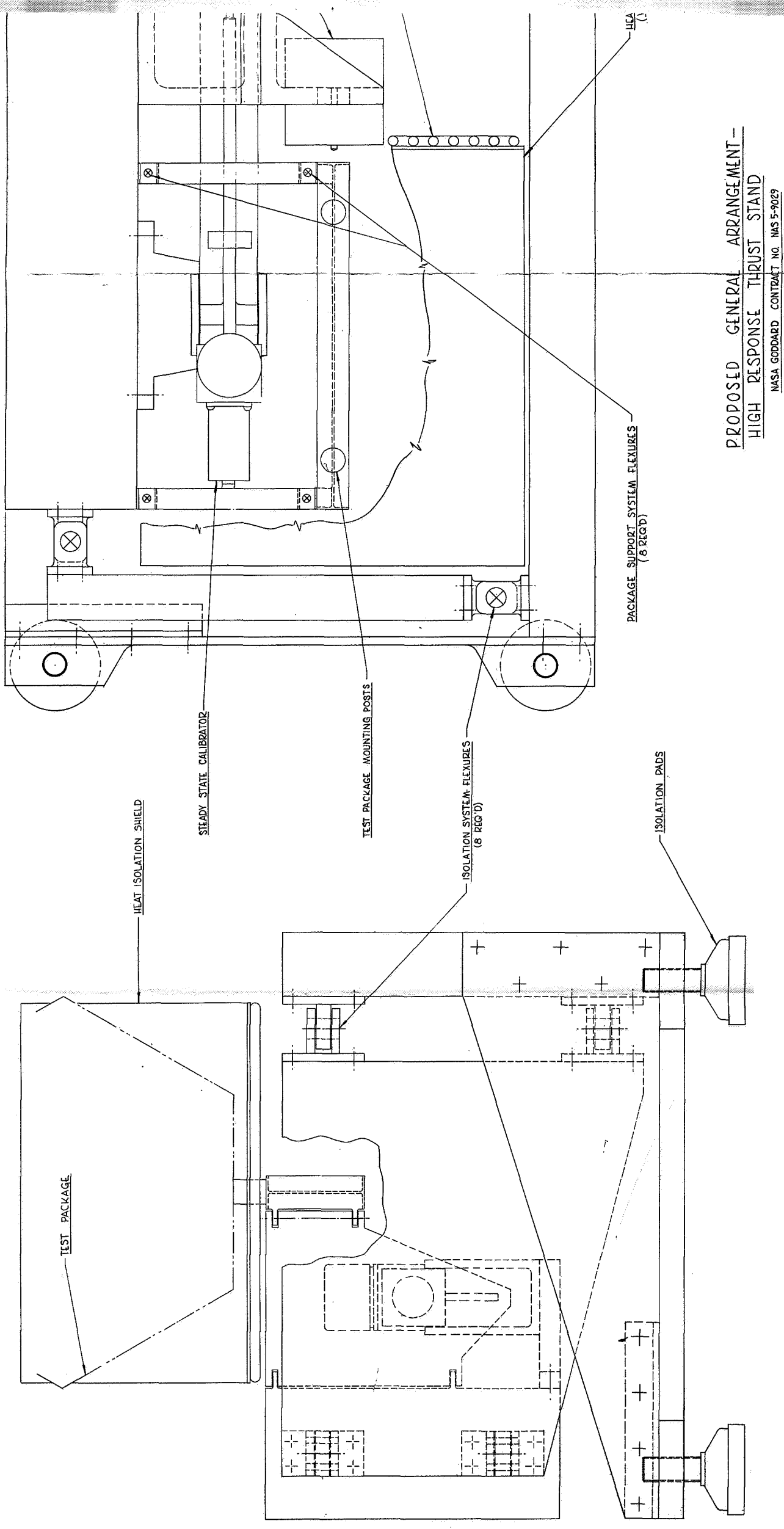


Fig A-5



PROPOSED GENERAL ARRANGEMENT -
HIGH RESPONSE THRUST STAND

NASA GODDARD CONTRACT NO. NAS 5-9029

TRANSducer & DAMPER

COOLANT LINES

ISOLATION SHIELD (WATER COOLED)

[illegible]

